Utrecht University

Deltares

Master's Thesis – Master Water Science and Management

The Operationalization of Resilience in Flood Risk Management

An Assessment Based on the Post-Hazard Using the Output of Hydrological Models and Publicly Available Global Data

Alice Ampolini

Student number: 5977339

Email: a.ampolini@students.uu.nl

Utrecht University supervisor: Dr. Jaivime Evaristo

Deltares supervisor: Hans Gehrels

18th July 2022

Summary

The frequency and magnitude of extreme weather events such as flooding is increasing due to climate change. Cities are hotspots to hazards such as flooding due to the growing population and the changing in lands that follows, placing an increasing number of people at risk for their lives and their possessions. Many post-2015 global agendas, such as the Sustainable Development Goals, are stressing the importance of risk assessment through the implementation of resilience measures with it. However, resilience is lacking a clear definition in the academic field and it is generally assessed with a qualitative approach, making its evaluation difficult. For these reasons, the aim of this thesis is to quantify urban resilience to flooding in one single value allowing better disaster management.

Four indicators describing urban resilience to flooding were chosen from literature and calculated using global open datasets and the output of hydrological models on the two case studies of Semarang and Vientiane. Once the quantification of the indicators was completed, these were inserted into an equation to obtain one single value of resilience allowing comparison between the two cities and the flood types. Through a sensitivity analysis the final values were tested to find the 95% confidence interval in which they were placed.

The analysis produced result in a range of values between 0 and 1, showing better hazard response for the city of Semarang over the case study of Vientiane, with higher flooding resilience value for the former over the latter.

Concluding, this thesis presents an innovative and reproducible methodology for the operationalization of resilience in urban environments allowing:

- Its inclusion into the risk assessment framework,
- Comparison between cities to support the more vulnerable ones,
- Recognition of fields of adaptation needing improvements.

Thus, the complementarity of risk and resilience can lead water managers and policy makers to gain a holistic view on the damages caused by the flooding and on the post-hazard, resulting in more equalitarian and efficient adaptation strategies.

Keywords: *resilience, flooding, risk assessment, water management, publicly available global dataset, hydrological model*

Contents

List of Appendix, Tables, and Figures:

1. Introduction

1.1 The impact of climate change on flooding

The current climate condition, highly affected by anthropogenic climate change, has led to "irreversible impacts as natural and human systems are pushed beyond their ability to adapt" (IPCC, 2022, p. 8). Experts, with the help of climate models, work on predictions that aim to indicate how the climate will impact the system Earth. Despite the results always containing a degree of uncertainty, experts have been observing a trend consisting of more frequent and severe extreme weather events all over the world (Weilnhammer et al., 2021). Extreme weather events according to Broska et al. (2020) refer to "a dynamic occurrence within a limited timeframe that impedes the normal functioning of a system or systems" (p. 115). The extreme weather event considered in this research is flooding, defined by Hutapea et al. (2020) as "a phenomenon that occurs when the intensity of rain that falls is very high, where the ability of absorption into the ground has been exceeded, resulting in runoff with the number and rate of large flow which can then become flooded" (p. 319). Additionally, flooding is referred to as a shock due to its sudden and often unexpected nature which generally develops in days (Mechler et al., 2019, Figueiredo et al., 2018). Flooding can be manifested in three different circumstances: coastal, fluvial and pluvial. In this thesis, the first one, coastal flooding concerns an excess of runoff due to the combination of high tides and storm events; secondly, fluvial flooding occurs due to an overflowing of the riverbanks which cannot be drained; and lastly, pluvial flooding is caused by heavy rainfalls which saturate the storage capacity of the drainage systems (Muthusamy et al., 2019).

Moreover, due to increasing migrations from rural to urban areas, cities are expanding at the expense of flood-prone areas (Ward et al., 2020). It is in fact estimated for the population living in urban environments to reach up to 68% of the total population by the year 2050 from the current 55% (Avashia & Garg, 2020). Urbanization is the number one factor that affects the increasing number of flooding events. Soil is substituted with impervious surfaces for infrastructures built to accommodate the population. Consequently, the infiltration capacity is drastically reduced weighing down the water that is discharged on the sewage system (Manola et al., 2019; Avashia & Garg, 2020). Additionally, the increasing number of infrastructures leads to an increment of temperature due to a phenomenon called urban heat islands (Mohajerani et al., 2017). The main danger of increasing temperature is the effect that this has on floods, increasing their intensity of 12% per degree Celsius (Manola et al., 2019). Floods are recurrent phenomena which bring destruction and lead to catastrophes. An example of the impact of flooding is found in China where a typhoon costed the lives of hundreds of people while many more were displaced (Brimicombe et al., 2021). Similar events manifested in America, the Caribbean and West Africa where the same extreme weather conditions led to many deaths (Brimicombe et al., 2021).

1.2 Global agendas

As a response to floods and to the recent catastrophes, global agendas highlight the urge for climate action. One example of the many is given by the Sustainable Development Goals (SDGs), 17 goals with the general aim of reducing poverty, enhancing living conditions and creating a sustainable future (UN, 2022). More specifically, goal 13 'Climate Action' defines indicator 13.1 by stating to "Strengthen resilience and adaptive capacity to climate-related hazards and natural disasters in all countries" (Figure 1) (UN, 2022), while goal 11, 'Sustainable Cities and Communities', with indicator 11.b points out the goal to "increase the number of cities and human settlements adopting and implementing integrated policies and plans towards inclusion, resource efficiency, mitigation and adaptation to climate change, resilience to disasters, and develop and implement holistic disaster risk management at all levels" (Figure 2) (UN, 2022). A call for risk reduction is therefore loud and clear, strengthening resilience as an approach to face it. Another agenda post-2015 is the Sendai Framework for Disaster Risk Reduction which, together with the SDGs and the Paris Agreement, call for resilience as a solution to pursue to reduce hazards, exposure

and vulnerability while supporting a fast response and, thus, recovery (De Bruijn et al., 2017; UNISDR, n.d.).

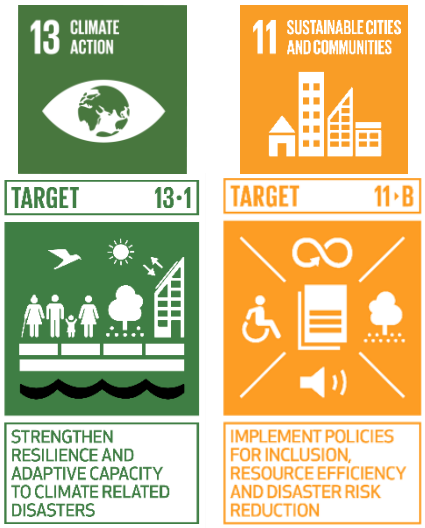

FIGURE 1: THE FIGURE ABOVE SHOWS SDG 13 – CLIMATE ACTION, AND SDG 11 – SUSTAINABLE CITIES AND COMMUNITIES WITH THEIR TARGETS 13.1 AND 11.B.

1.3 Resilience and risk assessments

De Bruijn et al. (2017) recall the term resilience as a "buzzword", rather than a practical concept, used in many fields and thus assuming different shades of meanings. Figueiredo et al. (2018) confirm that resilience is used mostly in the fields of social and natural sciences providing therefore 25 different definitions of the term. For instance, Holling in 1996, after using this concept for the first time in 1973, made a distinction between ecological and engineer resilience. The latter one is described as a type of resilience which "focuses on how fast a system returns to a steady state after a disturbance and how large the disturbance needs to be before a system is pushed out of its steady-state" (De Bruijn et al., 2017, p.22). The ecological interpretation of the term differs because it considers the ability of the system to cope and adjust according to the disturbance, so as to maintain a working system rather than reaching a steady state (Disse et al., 2020; De Bruijn et al., 2017). Similarly, Disse et al., (2020) touch upon the concept of social-ecological resilience which adds the participation of the community in constant change to adapt and hence address the conditions which led to a flooding event, capturing therefore the community in a "constant state of change" (p. 5). Finally, IPCC (2012) made a description of resilience which summarizes the definition as "the ability of a system and its component parts to anticipate, absorb, accommodate, or recover from the effects of a hazardous event in a timely and efficient manner, including through ensuring the preservation, restoration, or improvement of its essential basic structures and functions" (p. 5).

Despite the close relationship, risk and resilience have different assessments. Risk is often represented by the monetary damage on an area (Disse et al., 2020), and in literature (Luu and von Meding, 2018; Hagenlocher et al., 2018, Chan et al., 2021) it is often expressed as:

$$Risk = Hazard \times Exposure \times Vulnerability$$

Risk is directly related to the magnitude of the climate hazard, to the exposure of people that might be influenced by the hazard, and to the vulnerability of the people and surrounding environment. More specifically, hazard is defined by Hagenlocher et al. (2018) as an event or process that can lead to deaths and injuries, economical loss, and damage. Exposure covers the extent to which both people and infrastructures might be affected causing loss of lives and/or economic damages after a hazard (Hagenlocher et al., 2018). Lastly, vulnerability is the predisposition of people and infrastructure to be

affected by the hazard (Hagenlocher et al., 2018). Oftentimes, the quantification of risk is reported into climate risk indices. These are assessment tools made for a wide range of stakeholders representing both the global and the city level. The aim of indices varies from helping to improve urban management to the creation of a tool as a means for comparison by ranking different cities (Mavhura et al., 2017). Indices are normally composed of a set of multiple indicators which are aggregates of individual variables used as simplification of more complicated realities (Mavhura et al., 2017). An example is the Urban Climate Risk Index (UCRI), a fast tool under-development by Deltares which assesses the risk of flooding, drought, and heat stress throughout cities around the world using only globally available datasets (van Hemel, 2021; Blokland, 2021). However, a conventional critique to such indices, concerns the static condition that they bring (De Bruijn et al., 2017). In fact, the risk framework does not consider the possibility of including the response to different climate and socio-economic changes which, on the contrary, might reveal relevant information to disaster risk management (De Bruijn et al., 2017).

Resilience is often assessed using qualitative indicators. As for the risk analysis, indicators are useful to monitor the recovery response from shocks and to assess whether a goal has been met. Furthermore, the qualitative nature of the assessment provides the context to understand the extent on which a policy might or might not perform well through an in-depth analysis (Figureiredo et al., 2018). According to the OECD (Figureiredo et al., 2018), for a city to be resilient it is essential to have the capability to absorb, recover and be ready to face future shocks, hence favoring a new state of normality characterized by adaptation and dynamicity over stability. The main fields that require flexibility and adaptation are the economic, societal, governmental, and environmental dimensions. To acquire the level of flexibility industries should promote room for innovations, all the citizens should be included in an active society, the government must provide open and integrated long-term plans, and environmental sustainability must be achieved (Figureiredo et al., 2018).

This research focuses on urban resilience for flooding by studying the post-hazard response of cities through four indicators often used in literature (De Bruijn et al., under review), and quantifiable from global datasets. These are Distributional Impacts, Beyond Design Event, Welfare Loss, and Recovery Time. The first one, Distributional Impacts, concerns the equity in the distribution of a hazard, which may affect households and neighborhoods within each subdistrict to a different extent (Williams et al., 2020). For example, bigger houses tend to be less affected by the hazard, while the main consequences are often weighting on smaller households (Disse et al., 2020). This indicator is therefore relevant to make explicit who is affected the most to increase prevention and justifying additional compensating measures (De Bruijn et al., under review, Figureiredo et al., 2018). The second indicator, Beyond Design Event is based on the consideration of a single non-average hazard scenario. Blondel et al. (2021) stated that due to climate change more extreme and “rare” events, also called black swans, start to manifest with an increasing frequency bringing a high level of disturbance. An example of black swans are the flooding events that occurred in the summer of 2021 in the western part of Europe in which the flooding exceeded 1 in 100 years return period in multiple locations (Kreienkamp et al., 2021). The relevance of this indicator lays in the exploration of a catastrophic scenario to cover wide range of possible changes stimulating actions to reduce disastrous impacts and provide further knowledge for policy makers (De Bruijn et al., 2017, De Bruijn et al., under review). The third indicator covers Welfare Loss, the socioeconomical aspect of resilience, which describes to what extent poor areas are more severely struck by hazards, as more vulnerable communities take longer to recover (Walsh and Hallegatte, 2020, De Bruijn et al., under review). Risk assessment is often based on the monetary damages which do not count equally for all the people; therefore, this indicator shifts the focus to social-economic aspects such as income (De Bruijn et al., under review). Fourth and last, Recovery Time covers the capacity of the system to recover from overflows, assuming that flooded areas lose their functionality for as long as the event lasts (Bertilsson et al., 2019, De Bruijn et al., under review). Oftentimes, in fact, longer duration of floods triggers a series of indirect cascading events, some of which, for instance, might compromise access to primary infrastructure such as hospitals or emergency rooms (Bertilsson et al., 2019, De Bruijn et al., under review). Recovery Time is therefore strictly connected to both the damages caused by the hazard and the socio-economic

situation of the area affected by the flooding, since small damages and higher income allow a faster recovery (Leandro et al., 2020).

Finally, while risk assessment shows the damage at the time of the hazard, resilience completes the story by indicating what happens in the post-hazard. This view can lead to more efficient interventions and adaptation strategies for the vulnerable areas (Walsh and Hallegalle, 2020). However, this should not discourage the adoption of a risk assessment approach, but rather the integration of both (Disse et al., 2020).

1.4 Knowledge gap

Due to the wide definition of the term, resilience is often measured qualitatively (Disse et al., 2020, De Bruijn et al., 2017). For example, De Bruijn et al. (2017) developed a holistic approach to measure both risk and resilience in the municipality of Dordrecht (The Netherlands). The main strategy was to create storyline with notions that covered all the steps from before to the post-hazard event. This strategy resulted in more comprehensive measures which covered the occurrence of black swans and other variables such as land cover change (De Bruijn et al., 2017). Nevertheless, researchers have tried to look past the qualitative approach to quantify the concept of resilience for a specific case study to facilitate its inclusion into a risk assessment framework. Bertilsson et al. (2019), for instance, created the Spatialized Urban Flood Resilience Index (S-FRESI), a multicriteria index which focuses on the characteristic of the hazard, the system exposure and susceptibility and, finally, material recovery from the losses caused by the flooding event. In this case, however, the researchers needed specific data which was gathered from an in-depth study conducted in two theses to be able to quantify the monetary losses resulting from the flooding event (Bertilsson et al., 2019). This example shows that even though resilience can be assessed quantitatively, it is still a complex process due to the need of specific data which can only be gathered in situ through in-depth studies in current practice (Campbell et al., 2019). Hence, there is a gap in the literature of resilience when it comes to the quantification of urban flood resilience using only publicly available global data supported by the outcome of hydrological models.

1.5 Aim of the research

The intent of this research, conducted as a part of an internship at Deltares, is to ‘operationalize’ resilience, with operationalizing meaning to create a methodology to quantitatively assess post-hazard observations in a concrete and reproducible manner to help guide future policies. This was done starting from the quantification of the abovementioned indicators through publicly available global datasets in two case studies in Semarang (Indonesia), and Vientiane (Lao PDR). Following, the assessment proceeded by assigning one final value to flood resilience available for its inclusion in the traditional risk assessment. Therefore, the research question and the associated sub-questions that guided the study are the following:

How can urban resilience to flooding be operationalized using publicly available global data to be included in the risk assessment framework?

1) *How can the urban resilience indicators to flooding be quantified using publicly available global open datasets for the two case studies?*
2) *How can urban resilience to flooding be quantified in one final value representative of all its indicators?*

By answering the main research question, through its two sub-questions, an innovative and reproducible methodology able to operationalize and assess resilience in cities is created using a fast assessment approach. The additional value of this research in the water science and management field is to contribute to a better management of flooding through the inclusion of the post-hazard assessment to the more traditional risk management approach, starting from its evaluation. Additionally, the inclusion of resilience can have a relevant impact at the societal level too, leading to better and more inclusive

adaptation strategies to co-live with further future changes, shortening the distance to more flexible and dynamic environments.

2. Methods

2.1 Case studies description

Two case studies were chosen to address the quantification of the four indicators. These were: Semarang (Indonesia) and Vientiane (Lao PDR) (Figure 2). These cities were chosen because of the availability of data from previous Deltares' projects and their history of flooding events.

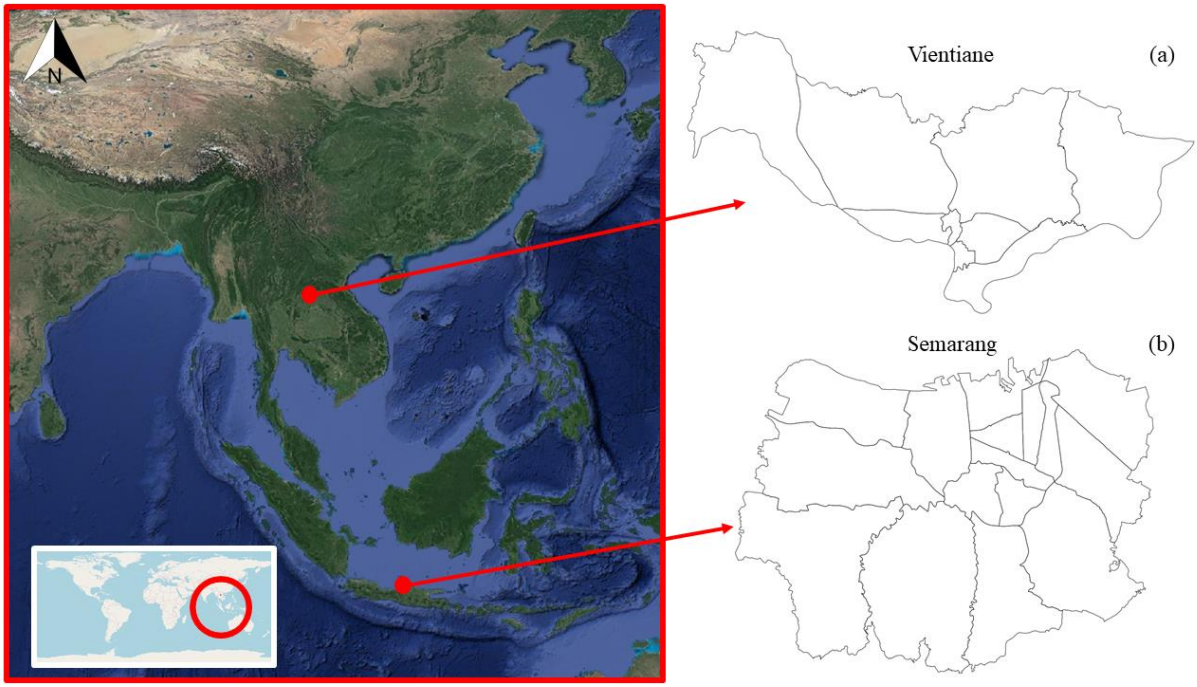

FIGURE 2: THE FIGURE SHOWS AN INSET OF THE GLOBE WITH THE EASTERN SIDE CIRCLED IN RED. THE EASTERN SIDE OF THE GLOBE IS THEN VISUALIZED WITH A SATELLITE VIEW IN WHICH THE TWO CASE STUDIES ARE INDICATED ON THE MAP WITH A RED DOT. FIGURE (A) AND (B) ARE AN ENLARGED REPRESENTATION OF THE CASE STUDIES OF VIENTIANE (A) IN LAO (PDR) AND SEMARANG (B) IN INDONESIA. BOTH THE CASE STUDIES (A, B) ARE REPRESENTED AT THE SUBDISTRICT LEVEL.

2.1.1 Semarang

Semarang is the capital of the Central Java Province, located in the northern part of the Java island in Indonesia (figure 2b), directly adjacent to the Java Sea (Harwitasari and van Ast, 2011). Morphologically the city is divided into a hilly area in the north, and a low-lying area in the south characterized by an elevation that varies between 0 to 25 meters above the sea level. The lower part is affected by land subsidence and settlement density, while the northern part has recently been affected by a problem of settlement caused by land cover change due to increasing urbanization (Kurniawan & Suharini, 2021). This led to a shift in the areas naturally employed as water catchment, reducing their hydrological contribution as water drainage and leading to increasing flooding. In fact, Semarang was recognized as a city prone to flood risk already in the Dutch colonial era, when the first canals were built to accommodate draining water (Kurniawan & Suharini, 2021). Moreover, because of its tropical climate characterized by constant rainfalls, and a growing population, the city is affected by pluvial, fluvial, and coastal flooding. The latter flood type is further triggered by a combination of sea level rise and land subsidence which

expanded the flood-prone area in the coastal region (Harwitasari and van Ast, 2011, Kurniawan & Suharini, 2021). In fact, more than half of the subdistricts of the city are currently threatened by the risk of flooding (Kurniawan & Suharini, 2021).

2.1.2 Vientiane

Vientiane is the capital of Lao PDR, located in the center of the country (Figure 2a), along the Mekong river. The city is characterized by a tropical climate which can be simplified in rainy seasons between the months of May and November and dry seasons from December to April with an annual average precipitation of 1660.5 mm (Sharifi et al., 2014, Sonnasinh, 2008). The city is prone to monsoon flooding of two different kinds: pluvial and fluvial, with pluvial flooding being the most common, while fluvial flooding is less frequent but with higher economic damages (Try et al., 2022, Sonnasinh, 2008). Scattered marshlands are a natural buffer to flooding, however the rapid urbanization that is affecting the city is putting them under threat making the city more vulnerable.

2.2 Data management

2.2.1 Software

Throughout the research Excel, RStudio, Python and QGIS were used for data preparation, manipulation, and visualization. More specifically, Excel was used to create a dataset during the quantification of the four indicators for the case studies and to perform the sensitivity analysis (Appendix D). RStudio was used to perform descriptive statistics to visualize the Distributional Impacts and the Beyond Design Event indicators and the result of the sensitivity analysis (Appendix E). QGIS was used during the manipulation of data for the Distributional Impact, Beyond Design Event and Welfare Loss and for the visualization of the Distributional Impacts indicator by creating maps (Appendix A). Furthermore, to perform the analysis of Beyond Design Event and Recovery Time, the model building software package HydroMT was used. HydroMT is an open source package running on Python developed by Deltares and used to build models by creating an automated workflow (Deltares, 2022). Two HydroMT plug-ins were used in the analysis, namely SFINCS and Delft-FIAT. The Super-Fast Inundation of CoastS (SFINCS) plug-in is a fast model that initially simulated the extent of only coastal inundation, while currently its adequacy increased to measure fluvial and pluvial flooding too (Leijnse, 2018). SFINCS was used in the research to quantify the Recovery Time and to simulate the pluvial flooding with 50 years return period in Semarang (Appendix B). The second plug-in is called Delft-FIAT, a model which calculates through a probabilistic approach the extent of damages to infrastructure starting from the exposure, the extent of the flood (SFINCS file) and the susceptibility of the area (De Bruijn, 2005; Slager et al., 2016). Delft-FIAT was used to calculate the damages during the quantification of the Beyond Design Event indicator (Appendix C).

2.2.2 Data collection

The input files for the research were divided into raster layers from hydrological models and open dataset. The former ones were retrieved from Dryad (Kummu et al., 2020), an openly available gridded dataset presenting the GDP PPP (Purchase Power Parity) on a global scale, and WorldPop (2022), another open dataset offering global gridded population data. The hydrological input files consisted of raster layers retrieved, when available (Table 1), from previous projects managed by Deltares, namely the Climate Risk in Cities, and the Baseline Study on Integrated Urban Flood Risk Management for Vientiane and Paksan Cities. More specifically, the input file for the Distributional Impacts and the Welfare Loss consisted of an existing raster layer produced by the Delft-FIAT model retrieved by the previous project. Similarly, the input files for the Beyond Design Event were raster layers generated by the model SFINCS from the available results of previous projects. An exception was made for the input file of the pluvial flooding of Semarang which, due to unavailability, was generated in this study based on historical data using SFINCS. Recovery Time was the indicator for which SFINCS was used to generate new input files. However, it is

relevant to mention that hydrological modeling was not the core of the methodology but rather a way to generate inputs and outputs used to give information on the response to the hazard by analyzing its post-scenario.

TABLE 1: THE TABLE BELOW SUMMARIZES THE INPUT FILES FOR THE QUANTIFICATION OF THE FOUR INDICATORS. THREE INDICATORS (DISTRIBUTIONAL IMPACTS, WELFARE LOSS, AND BEYOND DESIGN EVENT) USED AS INPUT RESULTS AVAILABLE FROM PREVIOUS PROJECTS, WHILE FOR ONE INDICATOR (RECOVERY TIME) NEW MODELS WERE CREATED IN THE CURRENT RESEARCH.

*EXCEPT FOR THE BEYOND DESIGN EVENT FOR PLUVIAL FLOODING IN SEMARANG WHICH WAS CREATED DURING THE CURRENT RESEARCH.

Indicator	Input
Distributional Impacts	Existing Delft-FIAT raster layer
Welfare Loss	Existing Delft-FIAT raster layer and open data
Beyond Design Event	Existing SFINCS raster layer* and open data
Recovery Time	New SFINCS model

Data preparation

To prepare the data before the processing (2.3 Objective Analysis), the shapefiles of the case studies were downloaded and prepared on QGIS at the subdistrict administrative level (Appendix A). Additionally, this research imposed as a boundary an extra geospatial dataset called Global Human Settlement Layer (GHSL) (Florczyk et al., 2019). The GHSL is an open and free dataset created by the European Union and developed according to methodology suggested by the United Nations to facilitate statistical comparisons of cities. GHSL was chosen as an appropriate boundary layer because it is people driven, defining cities according to the most functional urban locations (European Commission, 2022, Figureiredo et al., 2018, Florczyk et al., 2019). This step was followed for the quantification of Distributional Impacts, Beyond Design Event and Welfare Loss. The data preparation regarding the Recovery Time consisted of the extrapolation of 30 years (1981-2010) of precipitation (era5 – hourly, Hersbach et al. (2020)), discharge (glofas era3 v31, Harrigan et al. (2020)) and of coastal tides (gtsm_codec_reanalysis_hourly_v1, Muis at al., (2020)). Following, the dates of the highest historical peaks were identified to create a base model with either pluvial, fluvial or coastal forcings using SFINCS.

2.3 Objectives analysis

In this section a step-by-step explanation of the data processing is divided in two objectives corresponding to the sub-questions guiding this research. The following table (Table 2) describes the methods through their narrative and rationale. More details covering the technical aspects of the methodology can be found in the GitHub folder whose link is shared in the Appendices.

TABLE 2: THE TABLE IS ORGANIZED AROUND THE TWO RESEARCH OBJECTIVES NAMELY QUANTIFICATION OF THE RESILIENCE INDICATORS, AND QUANTIFICATION OF RESILIENCE IN ONE VALUE. IN EACH EXPLANATION THERE ARE STATED THE OBJECTIVE, THE APPROACH, AND THE RATIONALE.

Objective 1: Quantification of the indicators for resilience using open datasets on two case studies.	This objective allowed the indicators describing resilience to be operationalized through a methodology that resulted in values rather than in qualitative explanations (Figure 3). This first step created the workflow through which resilience could be operationalized and applied on the two case studies.
Approach/Method: To quantify resilience the indicators were approached singularly starting from Distributional Impacts (DI). The indicator was calculated through the superposition of a spatially distributed damages raster layer generated by Delft-FIAT on QGIS. This returned a map of the case study divided in subdistricts of the city reporting the sum of damages caused by the flooding. The	

result was then given by the median value of the sum of damages per capita, from which lower numbers correspond to a low resilience and vice versa, since low values mean little difference between the damages occurred amongst the subdistrict and hence, higher fairness.

Welfare Loss (WL) was calculated by the ratio between the total sum of damages retrieved from a Delft-FIAT raster layer for a standard event, and the GDP PPP of the city. The result showed the extent of the yearly GDP PPP that would be used to cover the damages caused by the event.

The third indicator was Beyond Design Event (BDE). This indicator was quantified by selecting one black swan event having a 50-years return period for pluvial, 100-year return period for fluvial and 1000-year return period for coastal flooding. The selected events were retrieved from raster layer generated by SFINCS and used as input for Delft-FIAT. The hydrological model created a second raster layer showing the spatially distributed damages caused by the black swan throughout the city. The indicator was then calculated by dividing the total sum of damages and the GDP PPP and it is be interpreted as the percentage of GDP PPP of the damages caused by the event.

The last indicator, Recovery Time (RT) was calculated on the assumption that the deeper the flooding the longer it takes for the area to recover. Therefore, flooding events were modeled through SFINCS to investigate the extent and the duration of the event. Following, the output was postprocessed to quantify the duration of time that the water took to decrease to the 10 cm threshold, identified by Bertilsson et al., (2019) as harmless. The quantification of the Recovery Time was then found by dividing the time needed to reach the threshold from the peak by the total event duration.
Finally, the last three indicators (WL, BDE and RT) have an indirect relation with the meaning of resilience since low resulting values indicate a highly resilient scenario.

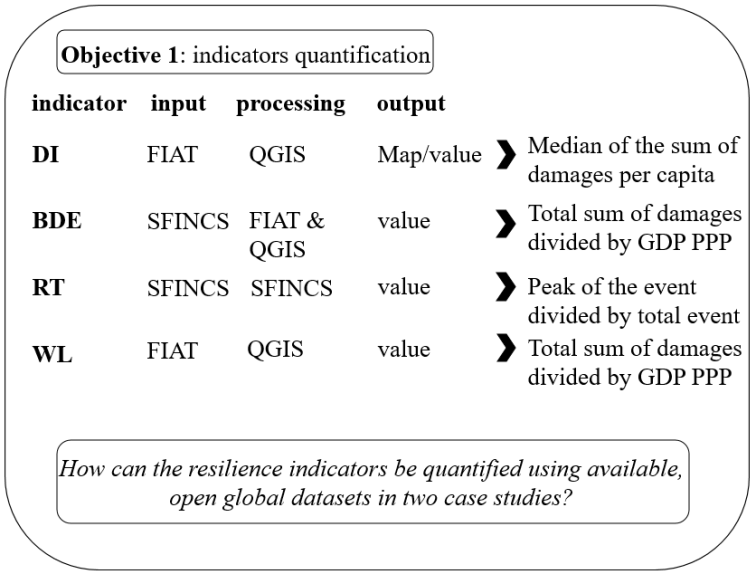

FIGURE 3: SCHEMATIZATION OF OBJECTIVE ONE (INDICATORS QUANTIFICATION). THE SCHEME SHOWS THE INDICATOR, ITS INPUT, PROCESSING, OUTPUT, AND A BRIEF DESCRIPTION OF THE SOLVING APPROACH. THE RELATIVE SUB QUESTION THAT WAS ANSWERED BY THE OBJECTIVE IS SHOWN IN THE BOTTOM PART OF THE SCHEME.

Objective 2: Quantification of resilience under one holistic value.	This was the final step of the research and consisted in defining one value to define resilience (Figure 4). This step concluded the research by answering to the second sub-question. The result of a single value for resilience is relevant for its inclusion in risk assessment calculation, allowing the flood analysis to be more complete while covering the damages caused by flooding hazards through a traditional risk assessment approach together with the post-disaster approach studied from the resilience indicators.

Approach/Method: The final resilience value was calculated following an equation similarly formulated by Bertilsson et al. (2019) and fitted for the current research, in which the indicators describing resilience are clustered together resulting in:

$$Resilience = DI \cdot m1 + (1 - WL) \cdot m2 + (1 - BDE) \cdot m3 + (1 - RT) \cdot m4 \qquad \text{(Equation 1)}$$

DI, BDE, WL and RT are the indicators, and *m1*, *m2*, *m3* and *m4* are the values inserted in the equation to give the possibility to weight each indicator according to the specific information and dynamics of each city. This allows space and flexibility to the end user to prioritize the specific indicator/s relevant for the case study (Figureiredo et al., 2018, Bertilsson et al., 2019). Additionally, a 1- was added to Beyond Design Event, Welfare Loss and Recovery Time to follow the logical concept of higher values indicating a high level of resilience which was not the case in the definition of these three aforementioned indicators. Finally, a sensitivity analysis was performed to analyze the change of the one resilience value when changing the weights coefficients of the formula.

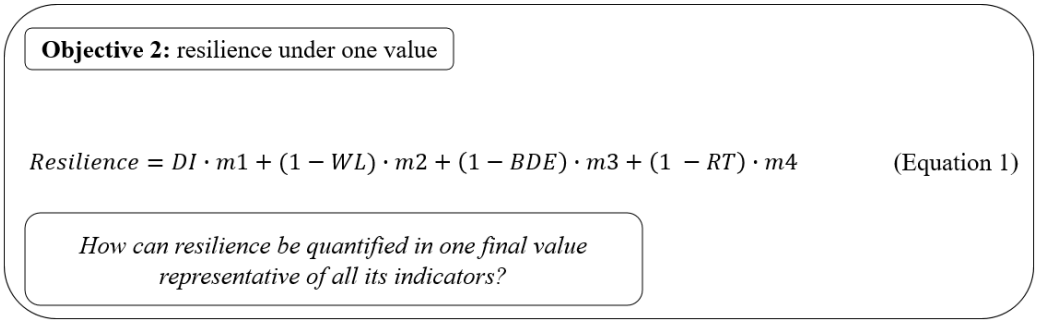

FIGURE 4: THE SCHEME SHOWS THE EQUATION (EQUATION 1) THAT WAS SOLVED IN OBJECTIVE TWO TO GET ONE HOLISTIC VALUE TO DESCRIBE RESILIENCE. AT THE BOTTOM THE SUB QUESTION THAT ANSWERS THE SECOND OBJECTIVE IS SHOWN.

2.4 Ethical issues

The results obtained by previous work used for the current project were operated for the creation of new results which consist of a cooperative work between Deltares and Utrecht University and stored in a protected folder located in the P-drive of the Deltares archive. Besides, other ethical issues do not apply to the current research.

3. Results

3.1 Objective 1

Each indicator was calculated following the methods mentioned in the previous section of this research. This first section aims at showing the results following the narrative of each indicator.

3.1.1 Distributional Impact

The Distributional Impact indicator provided spatial information of the distribution of damages affecting each subdistrict with flooding hazard. The damages were calculated in US dollars and visualized using QGIS to spatially show the variations of the damages through the subdistricts. The sum of damages per district per capita was then inspected through descriptive statistics to investigate its distribution. Finally, the indicator was quantified by calculating the median value for the sum of damages per district per capita. The final value therefore described the most frequent damages per capita falling in a range between 0 and 1, with lower values describing lower resilience and vice versa.

Semarang

In the first case study analyzed, the city of Semarang, the spatial distribution of the damages caused by a design event is observed in Figure 5.

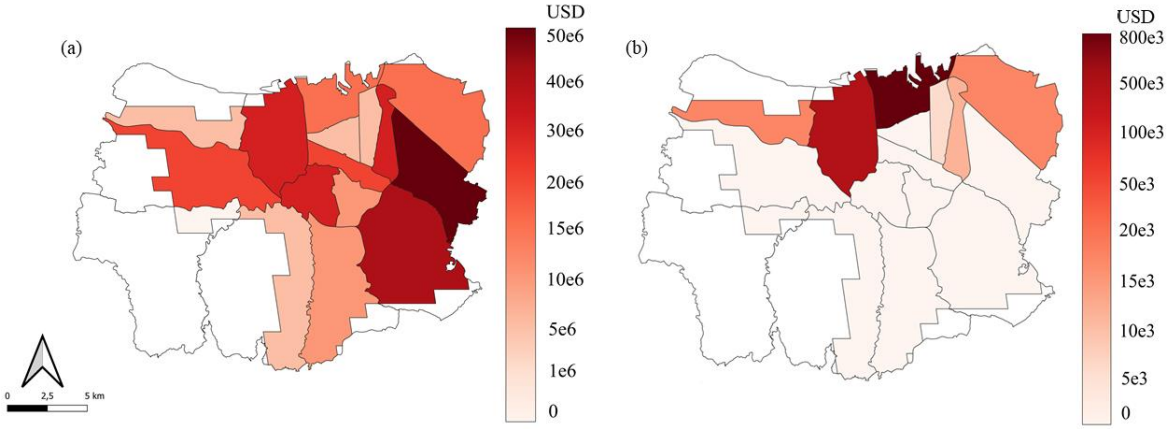

FIGURE 5: ABOVE, THE TWO MAPS SHOW THE DISTRIBUTION OF DAMAGES PER SUBDISTRICT OF PLUVIAL FLOODING (A) AND COASTAL FLOODING (B). BOTH MAPS PRESENT THE SHAPEFILES OF THE CITY WITH ITS SUBDISTRICTS TOGETHER WITH THE SUPERIMPOSITION OF THE BOUNDARY RETRIEVED FROM THE GHSL EUROPEAN DATABASE. THE SUBDISTRICT CONSIDERED IN THE ANALYSIS ARE THE ONES HAVING A SCALE OF REDS AS COLOR SHADING. BOTH THE IMAGES SHOW A LEGENDA TO THE RIGHT OF THE MAP TO SHOW THE AMOUNT OF DAMAGE CAUSED BY THE HAZARD. LOW DAMAGES ARE REPRESENTED BY LIGHT SHADING, WHILE HIGH DAMAGES ASSUME DARKER RED SHADES.

Fluvial flooding was not taken into consideration in this case study due to non-existing damages observed in the raster files taken from previous projects in the areas of interested, therefore coastal and pluvial flooding were analyzed. The maps show that both pluvial and coastal flooding cause damages within the GHSL boundaries of the city. However, the damages between the two floods are of a different reach, in fact, pluvial flooding shows higher damages ranging from 1’000’000 USD to 50’000’000 USD, with the most impacted subdistricts being the eastern ones, followed by the central areas. On the contrary, the damages caused by coastal flooding vary from 5’000 USD to 800’000 USD affecting only the coastal subdistricts with the central ones having most of the damages. As the maps show, the damages among the subdistricts vary considerably in both flooding scenarios. Figure 6 shows the medians and the distribution of the damages per district per capita. The median for pluvial flooding (Figure 6a) is 0.05, hence most districts’ share is 5% of the total sum of the damages per district per capita. On the other hand, the median for coastal flooding (Figure 6b) has a lower value of 0.03 meaning that the impact of coastal damages in coastal subdistricts is 3% of the total sum of damages per subdistrict per capita, and hence, showing a higher variation in the damages’ distribution. Low values, as in this case, represent a heterogenous distribution of flooding damages along the subdistrict which translates in low resilience.

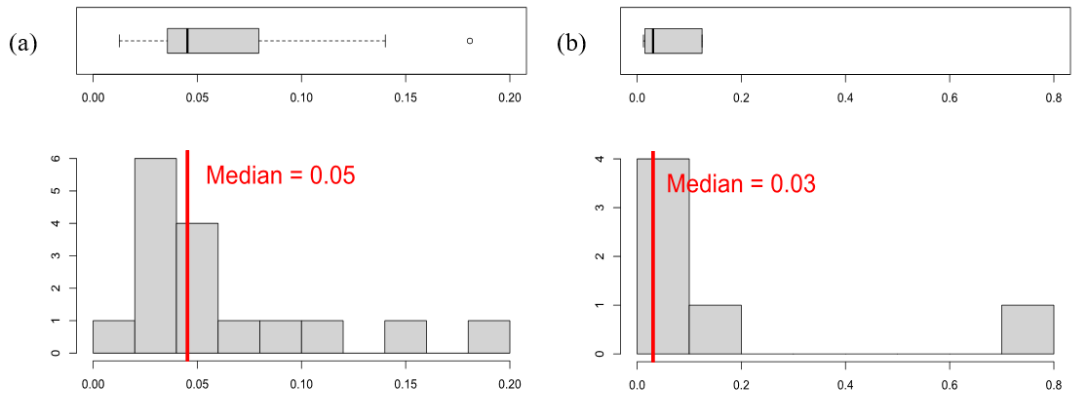

FIGURE 6: THE HISTOGRAMS, AND THE BOXPLOTS ABOVE, SHOW THE DISTRIBUTION OF THE PLUVIAL DAMAGES (A) AND COASTAL DAMAGES (B) PER CAPITA PER SUBDISTRICT. BOTH HISTOGRAMS PRESENT A SHAPE SKEWED TO THE LEFT SHOWING THAT THE MEDIAN FOR PLUVIAL FLOODING IS 5 %, WHILE THE VALUE BECOMES 3% FOR COASTAL FLOODING OF THE TOTAL SUM OF DAMAGES PER DISTRICT PER CAPITA**.**

Vientiane

The distributional damages of Vientiane are observed in the maps below (Figure 7).

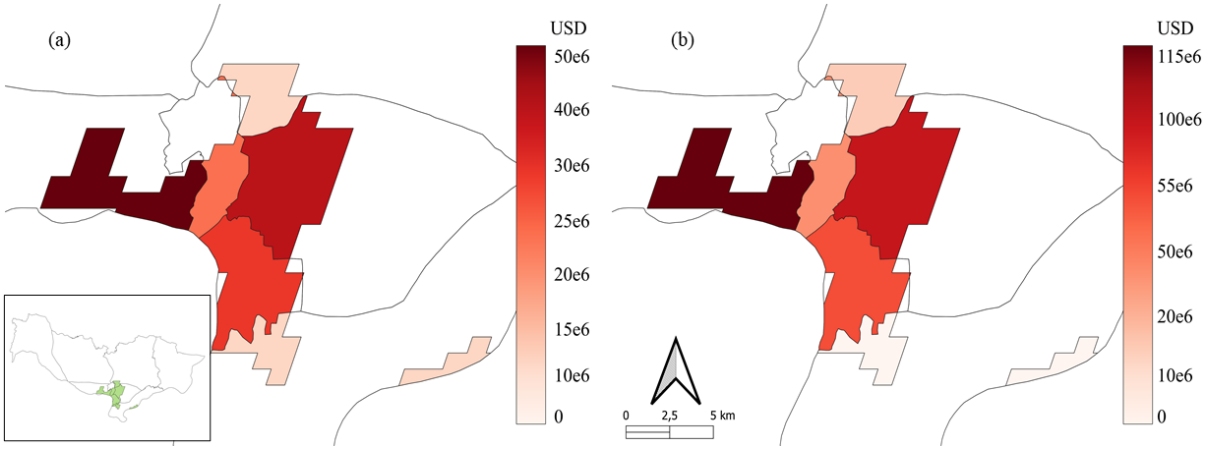

FIGURE 7: THE THREE MAPS ABOVE SHOW THE BOUNDARIES AND THE DISTRIBUTIONAL IMPACT FOR PLUVIAL AND FLUVIAL FLOODING IN VIENTIANE. MORE SPECIFICALLY THE INSET IN (A) SHOWS THE AREA OF VIENTIANE DIVIDED IN SUBDISTRICTS WITH THE SUPERIMPOSITION OF THE GHSL BOUNDARY USED IN THE RESEARCH. MAP (A) SHOWS THE DISTRIBUTION OF THE SUM OF DAMAGES PER SUBDISTRICT FOR PLUVIAL FLOODING WHICH RANGES FROM VALUES AROUND 10'000'000 USD AND 50'000'000 USD. (B), SHOWS THE DISTRIBUTIONAL SUM OF DAMAGES PER SUBDISTRICT FOR FLUVIAL FLOODING WHICH RANGES FROM VALUES AROUND 10'000'000 USD UP TO VALUES 10 TIMES LARGER.

The inset in Figure 7 shows that the population distribution according to the density within the GHSL boundaries concentrates only in the southern subdistricts adjacent the Mekong river, while the rest of the city is scarcely populated. Within the boundaries of the populated areas, both pluvial and fluvial floods generate damages. In fact, pluvial flooding (Figure 7a) shows damages up to 50'000'000 USD, while the value increases up to 115'000'000 USD in case of fluvial flooding (Figure 7b). In both instances the district that suffers the damages the most is the one located on the left side of the area, while the least affected districts are the upper and the lower ones. As the maps show, the damages are not distributed homogeneously since the impacts vary consistently amongst the subdistricts. This is also shown by the histograms and the boxplots in Figure 8. In fact, for both scenarios, most of the districts endure 15% of the

total sum of damages per capita in case of pluvial flooding (Figure 8a) and 12% in case of fluvial flooding (Figure 8b). These values show sign of higher homogeneity of the distribution of damages compared to the Semarang case study; therefore, their level of resilience concerning this indicator is higher.

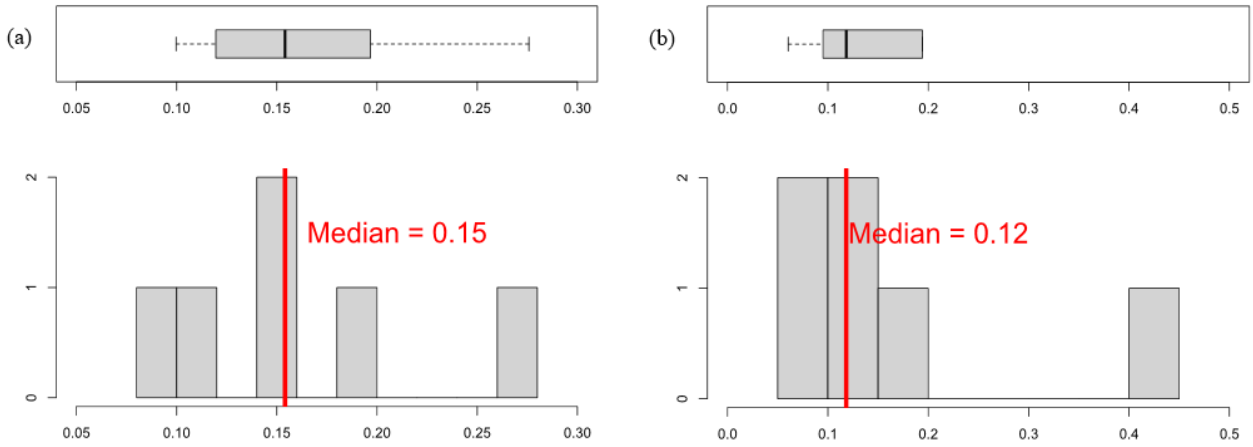

FIGURE 8: THE HISTOGRAMS AND THE BOXPLOTS ABOVE SHOW THE DISTRIBUTION OF THE DAMAGES PER DISTRICT PER CAPITA AND THEIR MEDIAN VALUES. THE MEDIAN FOR PLUVIAL FLOODING IN VIENTIANE IS 15% (A) WHICH MEANS THAT MOST OF THE SUBDISTRICT SHARE THE 15% OF THE SUM OF THE TOTAL DAMAGES PER CAPITA, WHILE THE NUMBER DECREASES AT 12% IN CASE OF FLUVIAL FLOODING (B).

3.1.2 Welfare Loss

The second indicator, Welfare Loss, provided information on the socio-economical response of the cities to the flooding hazards. It was calculated by dividing the total sum of the flooding damages by the total GDP PPP of the city. The total sum of damages was calculated by summing the damages per subdistrict obtained in the Distributional Impact, while the GDP PPP was retrieved from the Drayad global dataset. The GDP PPP stands for purchase power parity which compares the value of 1 US dollar to the value of the local currency. The result corresponded therefore to the percentage of GDP of the city in monetary damages caused by the hazard. A high resulting percentage explains that a considerable amount of the GDP would be spent on the event, while a lower percentage translates in smaller damages, hence, less money devoted to the flooding event.

For the case study of Semarang pluvial flooding resulted 3% of the GDP PPP, while coastal flooding was a low value considered to be approximately 0%.

In the case study of Vientiane pluvial flooding scored 4% of the GDP PPP, while fluvial flooding 6% of the total amount of GDP PPP.

Therefore, Semarang, by scoring lower values, resulted in a lower Welfare Loss than Vientiane. More specifically, coastal flooding was the most resilient flood type, while fluvial flooding in Vientiane resulted in it being the most expensive hazard analyzed.

3.1.3 Beyond Design Event

The third indicator, Beyond Design Event, provided information on the socio-economical response to a black swan event. The difference between Welfare Loss and Beyond Design event is thus the magnitude of the flooding event which for this indicator was extremized to study the response of the cities. The indicator was calculated by dividing the total sum of damages caused by the black swan by the GDP PPP. The black swan in the case of pluvial flooding was represented by an event with a return period of 50 years, while return periods of 100 and 1000 years were chosen for fluvial and coastal flooding respectively. The raster layers with the extent of the floods were generally retrieved from the Deltares archive. However, the extreme event for pluvial flooding was not available in the case of Semarang,

therefore the event was modeled from an historical event occurred in 2021 (Antara News, 2022) calculated as a 1 in 50 years return period event using SFINCS (Appendix B). To translate the extent of the flooding to the impact in damages the model Delft-FIAT was used. Its output was therefore a second raster layer showing the damages in the city caused by the black swan.

Finally, the quantified values for the Beyond Design Event indicator in Semarang were 0.16 and 0 for pluvial flooding and coastal flooding respectively. Similarly to the Welfare Loss, the results translate in 16% of the annual GDP PPP as the cost of the damages in case of extreme pluvial flooding, while, in case of coastal flooding the cost of the damages is approximately zero.

The final value for the quantification of this third indicator in Vientiane were 0.13 and 0.43 relatively for pluvial and fluvial black swans. Indicating higher costs to cover fluvial flooding damages.

To conclude, the most resilient scenario is coastal flooding in Semarang, following the same scoring obtained for the Welfare Loss indicator. The same counts for fluvial flooding in Vientiane which scored the highest score therefore being the least resilient scenario out of the studied ones. However, the scores of the pluvial scenario in the two case studies differs from the Welfare Loss with pluvial flooding in Vientiane scoring a lower value than pluvial flooding in Semarang, hence being more resilient.

3.1.4 Recovery Time

Recovery Time is the final indicator that describes flood resilience focusing on the temporal dimension. The indicator was calculated by dividing the time the water took to drain down to the 10 cm threshold by the total duration of the event.

Semarang Pluvial

In the case study of Semarang, the event (Figure 9) happened between the 01-02-2009 and 03-02-2009 was selected out of the 30 years (1981-2010) historical timeline because of its highest peak of precipitation which reached over 15 mm/h (Figure 9b). The maximum extent of the flooding for the event is shown in Figure 9a, together with the observation point (gauge) selected because of its incidence of high flood depth and high population density. The gauge registered the peak of precipitation in the chosen location (Figure 9c) with a peak that reached 1.85 m after three hours from the beginning of the event and stopped after 12 hours. The are underneath the curve of Figure 9c resulted approximately 12 meters-hour and it represents the water fell over the gauge during the duration of the peak, from its beginning to its end.

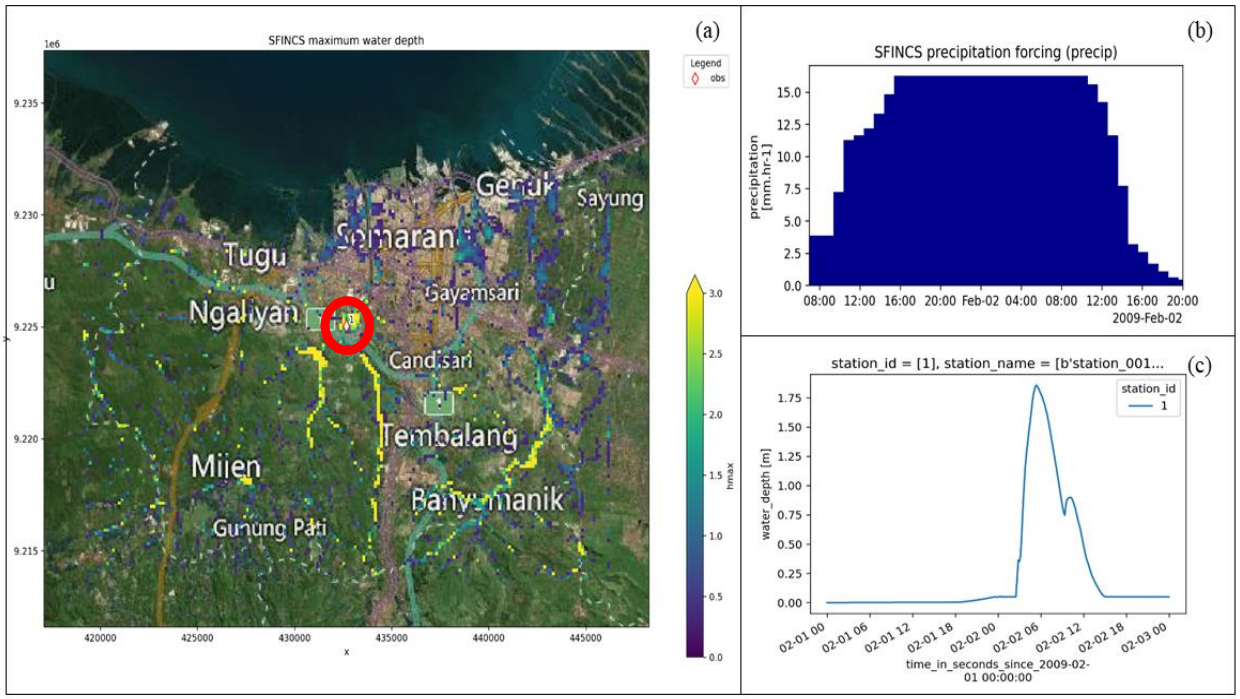

FIGURE 9: THE FIGURE IS COMPOSED BY THREE SUBFIGURES (A, B AND C) WHICH WERE USED TO CALCULATE THE RECOVERY TIME OF SEMARANG DURING THE MAXIMUM PLUVIAL EVENT EXTRACTED FROM A 30 YEARS SERIES. FIGURE 9A SHOWS THE MAXIMUM WATER DEPTH IN THE CITY OF SEMARANG. THE EXTENT GOES FROM 0 TO 3 METERS. HOWEVER, THE YELLOW AREAS CORRESPOND TO CANALS AROUND THE CITY, THEREFORE, THEY WERE NOT CONSIDERED AS MAXIMUM WATER DEPTHS POINTS. THE GAUGE IS THE DIAMOND SHAPE CIRCLED IN RED. FIGURE 9B SHOWS THE MAXIMUM PRECIPITATION FORCING EXTRACTED BY THE 30 YEARS' TIME-SERIES. THE PRECIPITATION IS MEASURED IN MM/H OVER THE DURATION OF THE EVENT STARTED ON 01-02-2009 AND ENDED ON THE 03-02-2009. FIGURE 9C SHOWS THE WATER LEVEL AT THE GAUGE LOCATION 1. X-AXIS SHOWS THE TIME WHILE Y-AXIS SHOWS THE WATER DEPTH IN METERS. THE PEAK BEGINS ON THE SECOND DAY AT 3 HOURS REACHING A MAXIMUM OF OVER 1.75 M 3 HOURS AFTER THE BEGINNING OF THE EVENT AND STOPS AT 15 HOUR OF THE SAME DAY.

The final value was obtained by counting the intervals of time from the peak of the event to the 10 cm threshold divided by the total duration of the event and it corresponds to 0.22 (Table 3).

TABLE 3: THE TABLE SHOWS THE VALUES USED TO QUANTIFY THE RECOVERY TIME INDICATOR FOR SEMARANG PLUVIAL FLOODING. IT PRESENTS THE START OF THE EVENT, THE END, ITS TOTAL DURATION, PEAK DURATION AND FINAL RECOVERY TIME RESULT.

Start event	01/02/2009 8:00 h
End event	02/02/2009 20:00 h
Total duration event	2160 min
Peak duration	530 min
Recovery Time	0.22

Semarang Coastal

The second forcing analyzed concerned coastal flooding for the event recorded in the first week of October 2005. The surge was selected out of 30 years (1981-2010) historical timeline because of the highest tidal peak which reached higher than 60 cm (Figure 10b). The corresponding map generated from the costal surge event (Figure 10a) does not show any trace of inundation depth. On the map an observation point (gauge) was selected because of its incident of humans' settlements and maximum flood. The peak registered by the gauge is shown in Figure 10c, and despite there was no sign of inundation, the water extent was investigated in more details. The gauge recorded in fact tidal behavior; however, its reach did not increase more than 26 cm, having a total time of submersion registering about 3 meters-hour (area of Figure 10c).

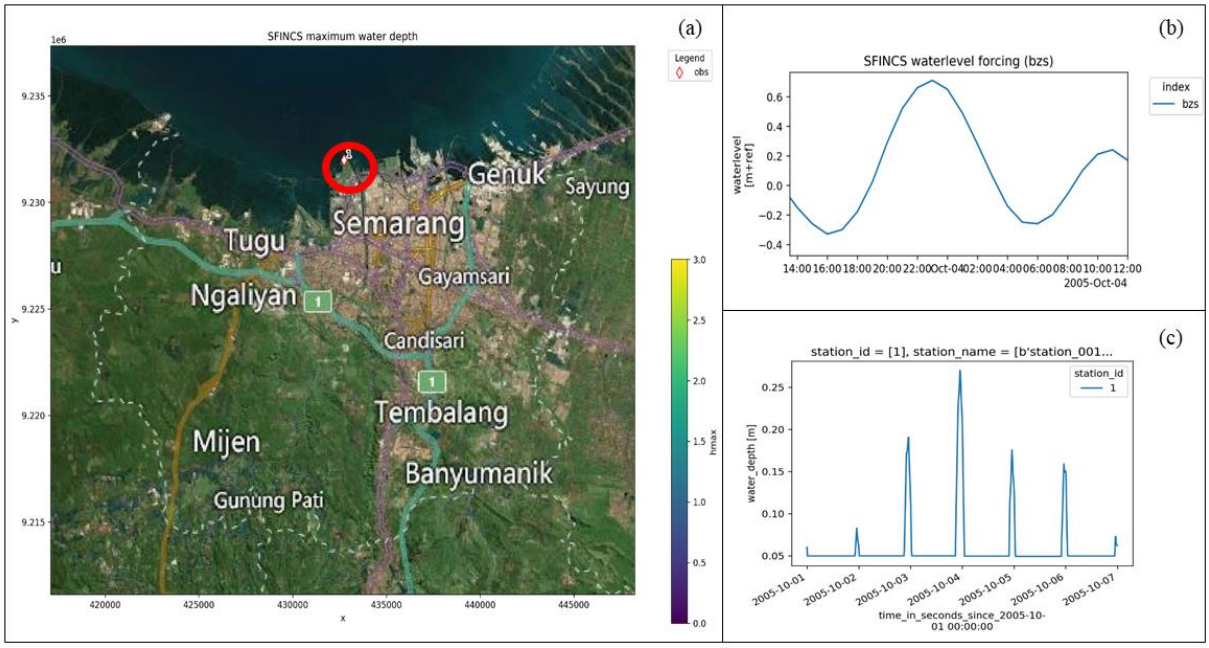

FIGURE 10: THE FIGURE IS COMPOSED BY THREE SUBFIGURES (A, B AND C) USED TO CALCULATE THE RECOVERY TIME OF SEMARANG DURING THE MAXIMUM COASTAL SURGE EVENT EXTRACTED FROM 30 YEARS HISTORICAL TIME SERIES. FIGURE 10A SHOWS THE MAP OF THE CITY OF SEMARANG (AREA LIMITED BY THE DOTTED LINE), NO INUNDATION WAS CAUSED BY THE FLOODING EVENT. THE EXTENT OF THE FLOODING REPRESENTED IN THE FIGURE GOES FROM 0 M (DARK BLUE) TO 3 M (YELLOW). THE GAUGE LOCATION IS SHOWN BY A DIAMOND SHAPE CIRCLED IN RED. FIGURE 10B SHOWS THE WATER LEVEL IN M OVER THE DURATION OF THE EVENT STARTED ON 01-10-2005 AND ENDED ON THE 07-10-2005. FIGURE 10C SHOWS THE WATER LEVEL AT THE GAUGE LOCATION. THE X-AXIS SHOWS THE TIME WHILE Y-AXIS REPRESENTS THE WATER DEPTH IN METERS. THE PEAK BEGINS BETWEEN THE 3RD AND THE 4TH OF OCTOBER REACHING A MAXIMUM OF 26 CM.

The final value was obtained by counting the intervals of time from the peak of the event to its end divided by the total duration of the event. The peak took 90 minutes to decrease from 26 cm to 10 cm, therefore 90 was divided by the duration of the event of 8 h (from 0 to the peak back to 0), hence the result of 0.19 (Table 4).

TABLE 4: THE TABLE SHOWS THE VALUES USED TO QUANTIFY THE RECOVERY TIME INDICATOR FOR SEMARANG COASTAL FLOODING. IT PRESENTS THE START OF THE EVENT, THE END, ITS TOTAL DURATION, PEAK DURATION AND FINAL RECOVERY TIME RESULT.

Start event	03/10/2005 19:00 h
End event	04/10/2005 03:00 h
Total duration event	480 min
Peak duration	90 min
Recovery Time	0.19

Vientiane Pluvial

The second case study, Vientiane, was analyzed for pluvial flooding during the peak event between 29-07-2001 and 01-08-2001 (Figure 11b). The peak was selected for being the highest precipitation in 30 years (1981-2010) historical timeline with a maximum peak of 7 mm/h. A map showing the maximum water depth relative to the chosen event is shown in Figure 10a together with 12 observation locations selected because of their incidence of high-water depth levels and high population density. More than one location was investigated in this case due to the behavior that the gauges recorded during the event (Figure 11c). In fact, the recorded water level varied between 0.2 and 1.75 m without any sign of decreasing to the 10 cm threshold during the total duration of the event. During the peak of the event the gauge registered about 24 meters-hour, corresponding to the area below gauge 7 in Figure 11c.

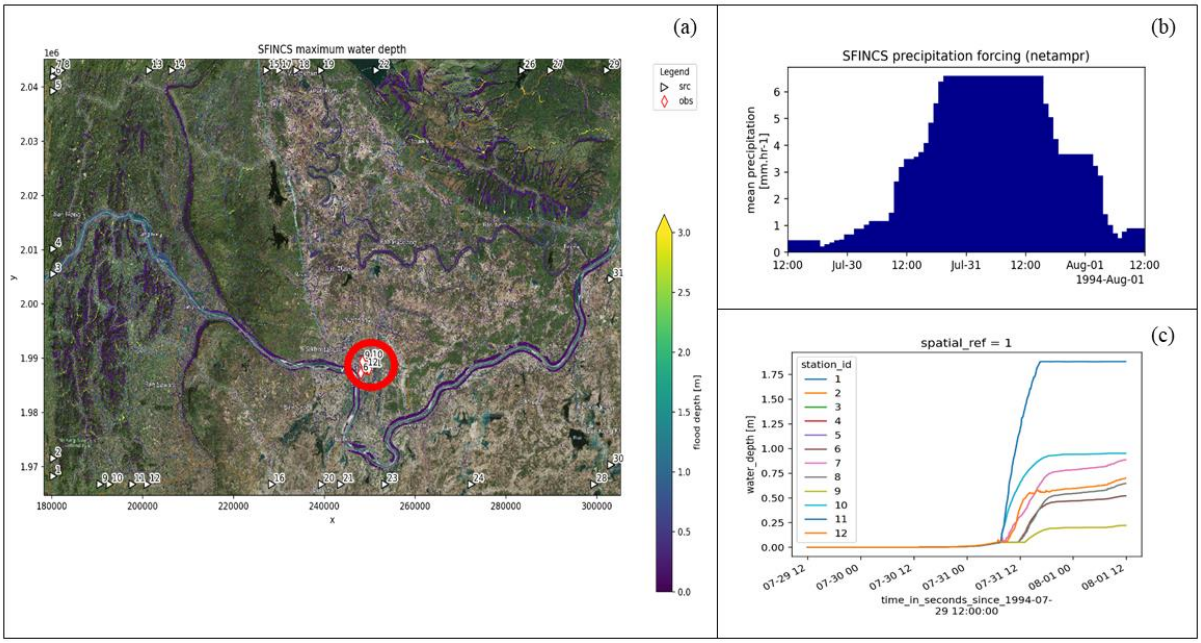

FIGURE 11: THE FIGURE IS COMPOSED BY THREE SUBFIGURES (A, B AND C) WHICH WERE USED TO CALCULATE THE RECOVERY TIME OF VIENTIANE DURING THE MAXIMUM PLUVIAL EVENT EXTRACTED FROM A 30 YEARS HISTORICAL TIME SERIES. FIGURE 11A SHOWS THE MAXIMUM WATER DEPTH OF THE CITY OF VIENTIANE. THE AREAS INUNDATED ARE MOSTLY AROUND THE RIVERS AND SPREAD IN THE MOST DENSELY POPULATED SUBDISTRICTS OF THE CITY. THE EXTENT OF THE FLOODING REPRESENTED IN THE FIGURE GOES FROM 0 M (DARK BLUE) TO 3 M (YELLOW). THE GAUGES LOCATIONS ARE PRESENTED BY A DIAMOND SHAPE CIRCLED IN RED, WHILE THE SRC TRIANGLES CORRESPOND TO AN INFLOWING RIVER DISCHARGE WHICH, HOWEVER, WAS NOT TAKEN INTO ACCOUNT IN THIS PART OF THE ANALYSIS. FIGURE 11B REPRESENTS THE WATER PEAK IN MM/H OVER THE DURATION OF THE EVENT STARTED ON THE 20-07-2001 AND ENDED ON THE 01-08-2001. THE PEAK REACHED THE 7 MM/H DURING THE 30TH OF JULY AND START DECREASING ON THE 31ST OF JULY. FIGURE 11C SHOWS THE WATER LEVEL AT THE GAUGES' LOCATIONS. X-AXIS SHOWS THE TIME WHILE Y-AXIS SHOWS THE WATER DEPTH IN METERS. THE PEAK BEGINS AFTER THE 31ST OF JULY AND DOES NOT SHOW SIGN OF DECREASING UP TO THE END OF THE EVENT.

The final value was obtained by counting the intervals of time from the peak of the event to its end divided by the total duration of the event. The peak took 23.3 hours with no signs of decreasing, therefore 23.3 was divided by the duration of the event of 60 hours, hence the result of 0.38 (Table 5).

TABLE 5: THE TABLE SHOWS THE VALUES USED TO QUANTIFY THE RECOVERY TIME INDICATOR FOR VIENTIANE PLUVIAL FLOODING. IT PRESENTS THE START OF THE EVENT, THE END, ITS TOTAL DURATION, PEAK DURATION AND THE FINAL RECOVERY TIME RESULT**.**

Start event	29/07/1994 18:00 h
End event	01/08/1994 06:00 h
Total duration event	3600 min
Peak duration	1398 min
Recovery Time	0.38

Vientiane Fluvial

Vientiane was analyzed for fluvial flooding during the peak discharge in the first two weeks of September 1995 (Figure 12). The peak was selected for being the highest discharge in 30 years (1980-2010) historical timeline with a peak of 26000 m3/s.

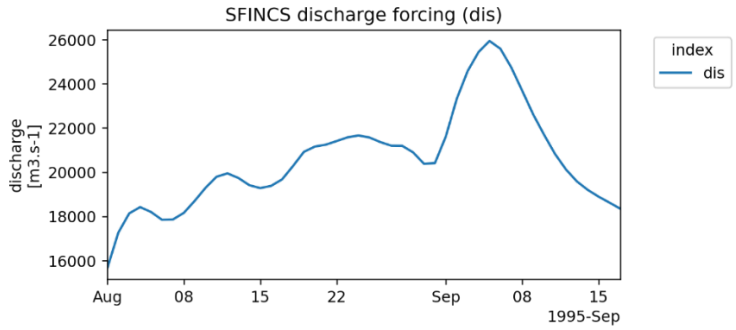

FIGURE 12: THE FIGURE REPRESENTS THE PEAK DISCHARGE IN M3/S OVER THE DURATION OF THE EVENT IN THE FIRST TWO WEEKS OF SEPTEMBER 1995. THE PEAK REACHED THE 26000 M3/S DURING THE 5TH OF SEPTEMBER.

During the running of the executable SFINCS, which determines the water depth and the extent of flooding, the model crashed returning the error that an overflow of 100 m is reached, therefore blocking the simulation. The error kept appearing during the multiple trial simulations, therefore, in this thesis the result was interpreted with the maximum and extreme value of 1.

To conclude, the table below (Table 6) summarizes the results obtained from the two case studies of Semarang and Vientiane concerning the flooding types that affect them.

TABLE 6: THE TABLE SUMMARIZES THE FOUR INDICATORS FOR RESILIENCE (DISTRIBUTIONAL IMPACT, WELFARE LOSS, BEYOND DESIGN EVENT AND RECOVERY TIME) QUANTIFIED FOR SEMARANG (PLUVIAL AND FLUVIAL FLOODING) AND VIENTIANE (PLUVIAL AND FLUVIAL FLOODING).

	Semarang		*Vientiane*	
Indicator	Pluvial Flooding	Coastal Flooding	Pluvial Flooding	Fluvial Flooding
Distributional Impact	0.05	0.03	0.15	0.12
Welfare Loss	0.03	0	0.04	0.06
Beyond Design Event	0.16	0	0.13	0.43
Recovery Time	0.22	0.19	0.38	1

3.2 Objective 2

Sensitivity Analysis

The aim of the last objective is to reduce resilience from four indicators to a single value. In doing so, Equation 1 was applied for pluvial, fluvial, and coastal flooding in the two case studies. The value resulting from the equation falls in a range between 0 and 1, with lower values indicating low resilience and higher values indicating a high resilience. Because of this reasoning a factor of '1-' was introduced in front of three indicators (Welfare Loss, Beyond Design Event, and Recovery Time) in which higher values resulted in low resilience and vice versa. Since the equation gives the flexibility to assign different weights to each indicator a sensitivity analysis was conducted to determine how the changes of weights influenced the final resilience value. At this scope, 100 series of different weights varying from 0 to 1, and adding up to 1, were generated on Excel obtaining 100 values of resilience per flood type. The distribution of the values was tested through descriptive statistics and a 95% confidence interval was investigate in RStudio. Figure 13 shows the result of the sensitivity analysis for Semarang and Vientiane.

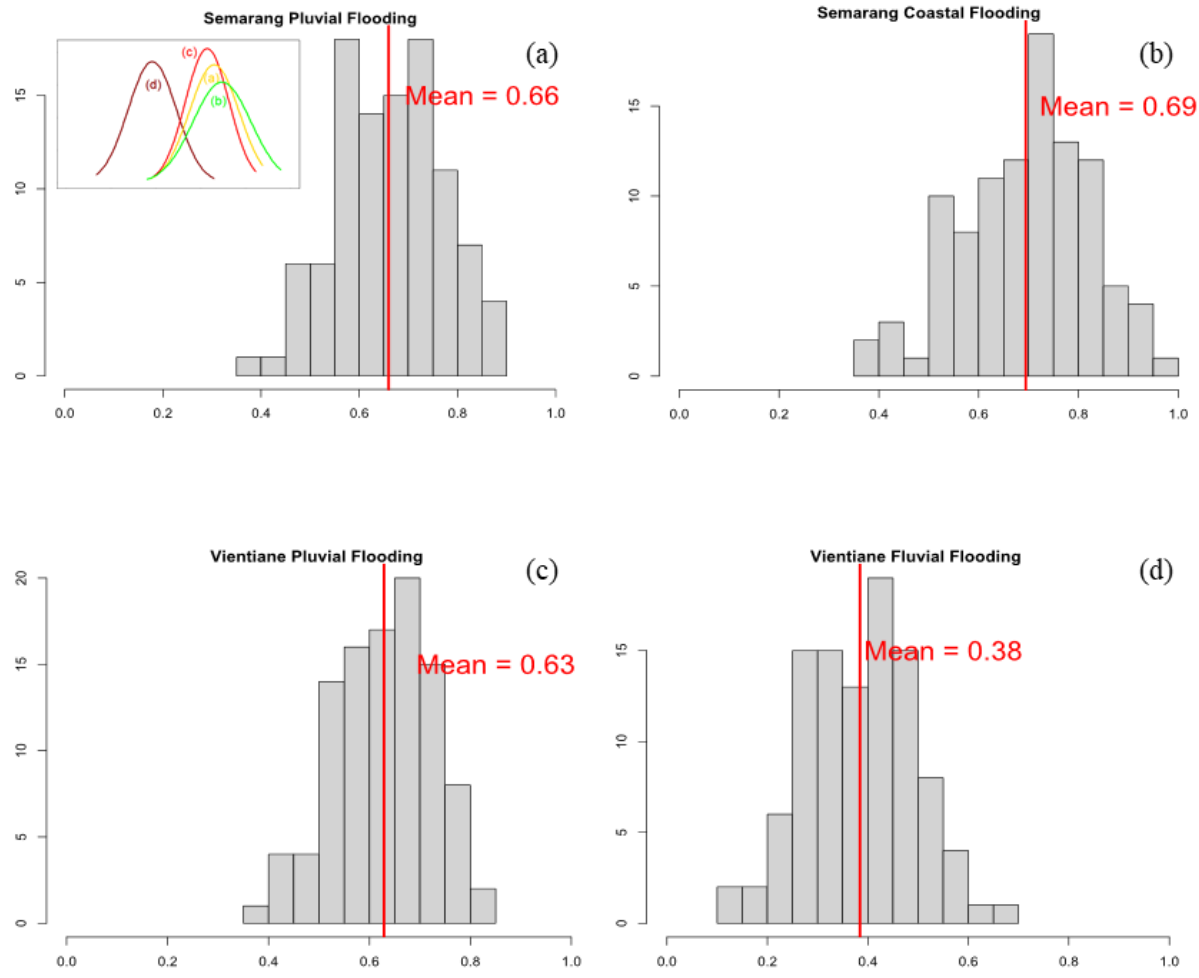

FIGURE 13: THE HISTOGRAMS ABOVE SHOW THE DISTRIBUTION OF THE VALUES FOR RESILIENCE AFTER THE VARIATION OF WEIGHTS IN THE SENSITIVITY ANALYSIS. FIGURE 13A SHOWS AN INSET WITH THE SUPERIMPOSED NORMALLY DISTRIBUTED CURVES OF THE CASE STUDIES (DARK RED FOR VIENTIANE FLUVIAL (D), RED FOR VIENTIANE PLUVIAL (C), YELLOW FOR SEMARANG PLUVIAL (A), AND GREEN FOR SEMARANG COASTAL (B)) AND THE HISTOGRAM FOR SEMARANG PLUVIAL WITH ITS MEAN OF 0.66. FIGURE 13B SHOWS THE HISTOGRAM FOR SEMARANG COASTAL WITH ITS MEAN OF 0.69. FIGURE 13C SHOWS THE HISTOGRAM FOR VIENTIANE PLUVIAL AND ITS MEAN OF 0.63. FIGURE 13D SHOWS THE HISTOGRAM FOR VIENTIANE FLUVIAL WITH ITS MEAN OF 0.38.

The results concerning the resilience values for Semarang are a mean of 0.66 with a 95% confidence interval between 0.64 and 0.68 for pluvial flooding and 0.69 with a 95% confidence interval between 0.69 and 0.72 for coastal flooding. Vientiane presented a mean value of 0.63 with a 95% confidence interval between 0.61 and 0.65 for pluvial flooding and a mean value of 0.38 with a 95% confidence interval between 0.36 and 0.41 for fluvial flooding. These results reported that Semarang has the highest value for coastal resilience towards flooding, followed by pluvial flooding, pluvial flooding for Vientiane, and finally fluvial flooding.

4. Discussion

4.1 Objective 1

The first results obtained from the study concerned the quantification of the Distributional Impacts indicator for the different flood types in the two case studies. Distributional Impact is the indicator that described the spatial distribution of the damages by looking at the median value of the share percentage of damages per district per capita. Therefore, low resulting values indicated a highly heterogeneity of the distribution of damages amongst subdistrict and hence lower equality in the monetary impact and a lower degree of resilience. In the case study of Semarang, the median value for pluvial flooding resulted 5% while coastal was 3%. This means that most of the subdistricts were impacted respectively by the 5% and 3% of the total damages per capita, and more specifically this variability is higher in the case of coastal flooding even when only the coastal subdistricts were chosen for this part of the analysis. Therefore, while most of the district were affected by low damages, few were highly impacted. Thus, even if the overall amount of damages was higher for pluvial flooding, the distribution resulted more homogeneous and, according to this indicator, more resilient. In the second case study, Vientiane, the overall distribution of damages results more homogeneous compared to Semarang. In fact, it scored 12% in case of fluvial flooding and 15% in case of pluvial flooding, meaning that most of the districts share those percentage out of the sum of damages per capita per subdistrict. In literature, Disse et al. (2020), pointed out the direct relationship between wealth and damages from which the higher heterogeneity of incomes the higher becomes the distribution of the costs of damages. While it is not yet clear whether higher damages strike on either poorer or wealthier people, it is proven that the wider range of damages affect scenarios with very different incomes. Following this logic, thus, it appears that the population of Semarang has more extreme diversity of incomes than Vientiane, whose districts reacted slightly more similar.

The second indicator quantified was Welfare Loss which described resilience under a socio-economical lens by comparing the total damages (at the city-level) of each flood type to the annual GDP PPP of the city. As De Bruijn et al. (2017) mentioned in their study, this indicator goes beyond the monetary losses often expressed by the risk assessment and focusses on the impact that the event would have on the annual GDP PPP. Furthermore, the damages are often described in USD, which has a relatively different value in different areas of the world. To avoid this inconvenience, the purchase power parity was adopted to translate the value of 1 USD to the value of the local currency. Under this indicator Semarang scored 3% and 0% respectively for pluvial flooding and coastal flooding. These results indicate that while a pluvial event would affect the city with damages comparable to 3% of the annual GDP PPP, the damages caused by coastal flooding would be negligible. On the other hand, Vientiane scored higher values such as 4% and 6% relatively to pluvial and fluvial flooding. The reasoning behind the difference concerns the lower GDP PPP of the city, and the higher damages that the two events would cause. Therefore, in this case as the Welfare Loss increases the resilience of the city decreases, indicating that its response is not adequate to buffer the damages.

Similarly, the Beyond Design Event described the socio-economical part of resilience by showing the response to a black swan event for the different flooding types. The relevance of assessing this indicator consists in informing policy makers of the expected damages that these events might lead to. Once again, the indicator was the result of the total sum of damages (at the city-level) divided by the annual GDP PPP. The result for pluvial flooding in Semarang increased steeply from a 3% to a 16%, while the result concerning coastal flooding remained stable to 0% suggesting only a small increment in the damages that the black swan would make. The city of Vientiane, instead, had a drastic increment in both pluvial and fluvial flooding with scores going from 4% and 6% up to 13% and 43%, almost half of the annual GDP PPP. The incremental results were expected as only the damages increased, while the GDP PPP remained constant.

The last indicator investigated in the research was Recovery Time. The indicator explored the temporal dimension to quantify the time that the water takes to drain from the peak to a safe threshold of 10 cm identified by Bertilsson et al. (2019). This indicator was calculated for the highest historical forcings, hence extreme events happened in a 30 years window between 1981-2010. The total duration of the event was quantified from its beginning to its end, while observation points registering the water depths were placed in locations with high density of human settlement. Therefore, the recovery time was calculated on the duration of the peak in those specific areas of interest (gauges). The ratio gave a value indicating the time that the water took to drain over the whole event, increasing therefore when the water would drain slower and decreasing with faster drainage. For the city of Semarang Recovery Time for pluvial flooding resulted 0.22 due to its peak decreasing over 8 hours from a maximum of 1.75 meters to 0.01 meter. Coastal flooding performed better with a result of 0.19 with the peak reaching 0.26 meters meaning that the water took longer than the pluvial scenario to drain down to the threshold. In the city of Vientiane, the Recovery Time was longer in the scenario of pluvial flooding scoring a value of 0.38. This was due to the fact that the pluvial water did not reach the threshold amongst the duration of the event, meaning that the water took a longer time to be drained and hence the maximum capacity of the infrastructures was not capable of coping with the flood (Bertilsson et al., 2019). In the case of fluvial flooding the resulting value was 1, indicating an extreme result. This was because the hydrological model (SFINCS) did not run correctly. In fact, it returned an error reporting a maximum inundation with an overflow of 100 m already from the beginning of the simulation. However, the results are validated by Try et al., (2022) and Sonnasinh (2008) who confirmed the drastic impact that fluvial flooding has on Vientiane. Additionally, Leandro et al. (2020) pointed out that higher income allows faster recovery, which can be observed in the case of Semarang where the city recovers faster and has a higher income.

4.2 Objective 2

Objective 2 consisted in solving Equation 1 which integrated the four indicators quantified in objective 1 and testing their weights through a sensitivity analysis. The equation can be unbuilt into four parts, one for each indicator. The first part, DI*m1, consisted of the value found for the Distributional Impact, a value from 0 to 1 for which smaller results suggested a low level of resilience and the relative weight. The second part, (1-WL)*m2, consisted in the Welfare Loss indicator which was subtracted to a unit value. This was done because low values indicated a higher degree of resilience, meaning that the event was compared to a smaller share of the GDP PPP. This was done to coherently and consistently find a final resilience value which translated in high resilience for values closer to 1 and low resilience for values closer to 0. For the same reasoning the following indicators (1-BDE)*m3 was subtracted to a unit too. Lastly, the final part of the equation (1-RT)*m4 was subtracted by the unit because higher values indicated a longer duration of time for the water to be drained back to a harmless depth.

Following, the weights were tested through a sensitivity analysis to investigate the change of the resilience value when the weights changed. To investigate this, 100 series of four values (corresponding to

m1, m2, m3 and m4) were generated and multiplied by the corrected indicators. The distribution of the results followed a normalized shape from which the mean and the 95% confidence interval were analyzed. The results indicated that, by means of comparison, Semarang has the most resilient response to coastal flooding with a result of 0.69, followed by pluvial flooding with a result of 0.66. The city of Vientiane scored for both scenarios lower values showing the lowest resilience of 0.38 for fluvial flooding, and a better response of 0.63 to pluvial flooding. For both the scenarios in the case study of Semarang the indicator that had the most positive influence on the final result was Welfare Loss, showing a stronger socio-economical response. On the other hand, the lowest indicator was found to be the Distributional Impacts which showed thus inequal responses amongst the subdistricts of the city. In the second case study, Vientiane showed higher results for the Welfare Loss indicator in both scenario, and lower in Distributional Impacts for pluvial flooding and in Recovery Time for fluvial flooding. In general, therefore, the socio-economical part of the resilience seemed to be the most robust for both the cities. However, it must be recognized that a standard event resulting 3% of the GDP PPP (Semarang pluvial) is still a very high monetary impact. Furthermore, in the case of fluvial flooding in Vientiane the lowest indicator resulted being Recovery Time for which it was already discussed that the model did not respond correctly, suggesting an error indicating low accuracy.

4.3 Implications

The results of this thesis can be addressed to stakeholders such as water managers and policy makers in three main points. Firstly, the quantification to the one holistic value of resilience can be introduced in the risk assessment framework creating an innovative approach. In fact, as Disse et al. (2020) stated, the complementarity of these two aspects gives the opportunity stakeholders to analyze the complete hazard event from its beginning to after its end conditions. Moreover, the quantitative approach can be completed by the qualitative assessment consisting of the explanation of the indicators from stakeholders to the broader audience. Furthermore, the inclusion of the resilience value might increase the accuracy of risk indices too, introducing the second point which consists in comparing cities using resilience as the main metric. By mean of comparison cities can be listed to distinguish the most vulnerable ones not as an act of discrimination, but rather as a way for readdressing climate fonds from international stakeholders to smaller realities (Figureiredo et al., 2018). Thirdly, the subdivision of resilience in singular indicators allows a novel overview of the fields on which cities are less prepared to face hazards. This can be done for instance by analyzing the indicators' lower scores to understand whether the infrastructures need better care to facilitate water to be faster drained, or if the economy must be pushed forward to front imminent black swans. This analysis has thus the power to bring different cities facing similar issues in new networks, sharing adaptation measures and strategies. Information becomes then of primary importance for city leaders, showing that resilience is not only a matter for researchers and academics, but it is a way to safely adapt to future changes that involve everyone.

4.4 Limitations and Future Research

According to De Bruijn et al. (2017), moving from a qualitative to a quantitative approach might cause information to be lost, or less clear. However, one approach should not eliminate the other. In fact, the scope of the quantification of resilience in this research was about creating a methodology able to measure the level of resilience of a city, and hence, to change the traditional qualitative scope of the analysis bringing new prospective on the table that can be integrated. In this paragraph a list of aspects that limited the research is presented, nevertheless, the results showed that the model developed can potentially be used to assign a direction for stakeholders such as urban planners.

The main limitation of this research relates to the definition of resilience itself. As it can be seen in the introduction, resilience assumes multiple meanings according to the field of application and the author who defines it. Therefore, it is relevant to understand that this research refers to the concept of resilience as

it is described by the indicators evaluated in the methods. Further research might assign resilience a universal definition, however, this has not happened yet, thus, end users must be aware of the specific definition of resilience acquired for this study before adopting this methodology. Furthermore, the adoption of specific and defined indicators decreases the level of ambiguity while narrowing down the broader sense of flood resilience for urban environments (Figureiredo et al., 2018).

Following, limitations concerning the indicators must be analyzed too. For instance, the Distributional Impacts assumes that an equality of damages leads to a higher degree of fairness amongst the subdistricts. This means that by not having the same damages people might be subjected to higher damages than others, assuming that people have larger possessions and hence differences in income. Some studies (Disse et al., 2020) refer to the fact that damages tend to be higher in richer areas whereas poorer districts having less possessions might be less economically damaged but more affected regardless. However, this assumption must be checked with more in-depth studies since the opposite might prove true as well in case wealthier districts had technological more advance adaptation to mitigate the impact of damages.

Secondly, a limitation concerning the Beyond Design Event indicator is that the period of the extreme events was chosen on the base of already existing raster layers of extreme events. While this solution offered a concrete view on the response to black swans, future research might create a standard event designed for higher forcings found from risk curve analysis, by for example choosing the return period following the safety standard level of the events.

Moving on to the Recovery Time indicator limitations, observation points were placed in populated areas to find the maximum recovery time; however, future research might expand the number of gauges to the whole gridded area to find more accurate values. Moreover, it was often the case in which one event led to the next one making it more complicated to recognize whether the runoffs were separated from each other. Therefore, more studies might focus on this separation to increase the accuracy of this indicator.

In general future research might want to decrease the limitations of this study while validating future results. This might be done for instance by coupling the results with local data and in-depth studies. Moreover, depending on the application of the end user of this methodology, the research might be reproduced at a courser level such as subdistricts, allowing thus further narrowed down information. Finally, this is a simplified model to evaluate and quantify resilience and, as all the models, it might contain errors and uncertainties.

5 Conclusion

The main research question driving this thesis is:

“*How can urban resilience to flooding be operationalized using publicly available global data to be included in the risk assessment framework?”*

The answer is that resilience can be quantified through indicators describing different aspects of the field by using globally available open datasets and outputs from hydrological models. The research, therefore, contributed to the broader water science and management field in the operationalization of flood resilience in urban environments. With its evaluation the flood disaster management can become more efficient for two reasons. Firstly, by including resilience in the flood risk assessment it is possible to learn what happens after the flooding occurs. Secondly, the quantification of resilience can be implemented in climate risk indices which work as fast assessment tools able to guide a broad range of stakeholders, such as water managers and policy makers, into the further implementation of climate measures. Thus, the

operationalization of resilience could offer broader and more complete view on the field of disaster management. How to include resilience in the risk assessment is something that is suggested as a topic for future research, however, the inclusion will complement the information available from the risk assessment framework once more case studies have been analyzed.

6 References

Antara News. (2022). Semarang's Flooding Caused By Extreme Rainfall, Tidal Flooding: Govt. https://indonesiatribune.com/2021/02/07/semarangs-flooding-caused-by-extreme-rainfall-tidal-flooding-govt/

Avashia, V., & Garg, A. (2020). *Implications of land use transitions and climate change on local flooding in urban areas: An assessment of 42 Indian cities*. https://doi.org/10.1016/j.landusepol.2020.104571

Bertilsson, L., Wiklund, K., de Moura Tebaldi, I., Rezende, O. M., Veról, A. P., & Miguez, M. G. (2019). Urban flood resilience – A multi-criteria index to integrate flood resilience into urban planning. *Journal of Hydrology*, *573*(June 2018), 970–982. https://doi.org/10.1016/j.jhydrol.2018.06.052

Blokland, P. J. (2021). Challenges, practices, and politics in assessing climate risks in cities by means of a global index. A case study on the Urban Climate Risk Index. Utrecht University.

Blondel, L., Paterson, I. G., Bentzen, P., & Hendry, A. P. (2021). Resistance and resilience of genetic and phenotypic diversity to "black swan" flood events: A retrospective analysis with historical samples of guppies. *Molecular Ecology*, *30*(4), 1017–1028. https://doi.org/10.1111/mec.15782

Brimicombe, C., Di Napoli, C., Cloke, H., & Wanzala, M. (2021). Guest post: Reviewing the summer of extreme weather in 2021. https://www.carbonbrief.org/guest-post-reviewing-the-summer-of-extreme-weather-in-2021

Broska, L. H., Poganietz, W. R., & Vögele, S. (2020). Extreme events defined—A conceptual discussion applying a complex systems approach. *Futures*, *115*(November 2019), 102490. https://doi.org/10.1016/j.futures.2019.102490

Campbell, K. A., Laurien, F., Czajkowski, J., Keating, A., Hochrainer-Stigler, S., & Montgomery, M. (2019). First insights from the Flood Resilience Measurement Tool: A large-scale community flood resilience analysis. *International Journal of Disaster Risk Reduction*, 40. https://doi.org/10.1016/j.ijdrr.2019.101257

Chan, F. K. S., Yang, L. E., Scheffran, J., Mitchell, G., Adekola, O., Griffiths, J., Chen, Y., Li, G., Lu, X., Qi, Y., Li, L., Zheng, H., & McDonald, A. (2021). Urban flood risks and emerging challenges in a Chinese delta: The case of the Pearl River Delta. *In Environmental Science and Policy* (Vol. 122, pp. 101–115). Elsevier Ltd. https://doi.org/10.1016/j.envsci.2021.04.009

Cornwall, W. (2021). Europe's deadly floods leave scientists stunned. *Science*, *373*(6553), 372–373. https://doi.org/10.1126/science.373.6553.372

De Bruijn, K., Buurman, J., Mens, M., Dahm, R., & Klijn, F. (2017). Resilience in practice: Five principles to enable societies to cope with extreme weather events. *Environmental Science and Policy*, *70*, 21–30. https://doi.org/10.1016/j.envsci.2017.02.001

De Bruijn, K. M. (2005). Resilience and flood risk management: a systems approach applied to lowland rivers.

De Bruijn et al. (submitted to “Nature Communications Earth & Environment"). Preventing floods from turning into disasters: adopting a resilience lens.

Deltares. (2022). HydroMT: Automated and reproducible model building and analysis. https://deltares.github.io/hydromt/latest/

Disse, M., Johnson, T. G., Leandro, J., & Hartmann, T. (2020). Exploring the relation between flood risk management and flood resilience. *Water Security*, *9*(January), 100059. https://doi.org/10.1016/j.wasec.2020.100059

European Commission. (2022). GHSL - Global Human Settlement Layer - Open and free data and tools for assessing the human presence on the planet. https://ghsl.jrc.ec.europa.eu/degurba.php

Esri. (2016). What is a shapfile? https://desktop.arcgis.com/en/arcmap/10.3/manage-data/shapefiles/what-is-a-shapefile.htm

Figueiredo, L., T. Honiden and A. Schumann (2018), "Indicators for Resilient Cities", OECD Regional Development Working Papers, No. 2018/02, OECD Publishing, Paris. https://doi.org/10.1787/6f1f6065-en.

Florczyk, A. J., Melchiorri, M., Orbane, C., Schiavina, M., Maffenini, M., Politis, P., Sabo, S., Freire, S., Ehrlich, D., Kemper, T., Tommasi, P., Airaghi, D., & Zanchetta, L. (2019). Description of the GHS Urban Centre Database 2015. In *Luxembourg: Publications Office of the European Union, 2019* (Issue February). https://doi.org/10.2760/037310

Hagenlocher, M., Renaud, F. G., Haas, S., & Sebesvari, Z. (2018). Vulnerability and risk of deltaic social-ecological systems exposed to multiple hazards. *Science of the Total Environment*, *631–632*, 71–80. https://doi.org/10.1016/j.scitotenv.2018.03.013

Harrigan, S., Zsoter, E., Alfieri, L., Prudhomme, C., Salamon, P., Wetterhall, F., Barnard, C., Cloke, H., and Pappenberger, F.(2020). GloFAS-ERA5 operational global river discharge reanalysis 1979–present, Earth Syst. Sci. Data, 12, 2043–2060, https://doi.org/10.5194/essd-12-2043-2020.

Harwitasari, D., & van Ast, J. A. (2011). Climate change adaptation in practice: People’s responses to tidal flooding in Semarang, Indonesia. *Journal of Flood Risk Management*, 4(3), 216–233. https://doi.org/10.1111/j.1753-318X.2011.01104.x

van Hemel, G. (2021). Assessing climate risks in cities worldwide. Utrecht University.

Hersbach, H, Bell, B, Berrisford, P, et al. (2020). The ERA5 global reanalysis. *Q J R Meteorol Soc*; 146: 1999– 2049. https://doi.org/10.1002/qj.3803

Hutapea, S., Maas, A., Jayadi, R., Faculty, A., & Mada, U. G. (2020). *Contents available at ISC and SID Journal homepage : www.rangeland.ir Biophysical Characteristics of Deli River Watershed to Know Potential Flooding in Medan City , Indonesia*. *10*(3), 316–327.

IPCC. (2012). Managing the Risks of Extreme Events and Disasters to Advance Climate Change Adaptation: Special Report of the Intergovernmental Panel on Climate Change. Cambridge, England: Cambridge University Press. https://doi.org.10.1136/jech-2012-201045.

IPCC. (2022). Summary for policy makers: Impacts Adaptation and Vulnerability. https://report.ipcc.ch/ar6wg2/pdf/IPCC_AR6_WGII_SummaryForPolicymakers.pdf

Kreienkamp, F., Philip, S. Y., Tradowsky, J. S., Kew, S. F., Lorenz, P., Arrighi, J., … L Otto, F. E. (2021). Bert Van Schaeybroeck 13 , Robert Vautard 5 , Demi Vonk 8 , Niko Wanders 12 1-Deutscher Wetterdienst (DWD). In *Royal Netherlands Meteorological Institute (KNMI)* (Vol. 13). Retrieved from Deutscher Wetterdienst website: https://www.meteo.be/fr/infos/actualite/ce-que-lon-sait-sur-les-pluies-

Kummu, Matti; Taka, Maija; Guillaume, Joseph H. A. (2020), Data from: Gridded global datasets for Gross Domestic Product and Human Development Index over 1990-2015, Dryad, Dataset, https://doi.org/10.5061/dryad.dk1j0

Kurniawan, E. & Suharini, E. (2021). Flood Disaster in Semarang City from Colonial to Reformasi: A Review of its Management. *Paramita: Historical Studies Journal*, 31 (2), 184-193. http://dx.doi.org/10.15294/paramita.v31i2.22879

Leandro, J., Chen, K. F., Wood, R. R., & Ludwig, R. (2020). A scalable flood-resilience-index for measuring climate change adaptation: Munich city. *Water Research*, 173. https://doi.org/10.1016/j.watres.2020.115502

Leijnse, T. (2018). SFINCS (Version latest) [Model]. Retrieved from https://sfincs.readthedocs.io

Luu, C., & von Meding, J. (2018). A Flood Risk Assessment of Quang Nam, Vietnam Using Spatial Multicriteria Decision Analysis. *Water*, 10(4), 461. MDPI AG. Retrieved from http://dx.doi.org/10.3390/w10040461

Manola, I., Steeneveld, G. J., Uijlenhoet, R., & Holtslag, A. A. M. (2020). Analysis of urban rainfall from hourly to seasonal scales using high-resolution radar observations in the Netherlands. *International Journal of Climatology*, *40*(2), 822–840. https://doi.org/10.1002/joc.6241

Mavhura, E., Manyena, B., & Collins, A. E. (2017). An approach for measuring social vulnerability in context: The case of flood hazards in Muzarabani district, Zimbabwe. *Geoforum*, *86*(October), 103–117. https://doi.org/10.1016/j.geoforum.2017.09.008

Mechler, R., Bouwer, L. M., Schinko, T., Surminski, S., & Linnerooth-Bayer, J. (2019). Loss and damage from climate change: Concepts, methods and policy options (p. 557). *Springer Nature*.

Mohajerani, A., Bakaric, J., & Jeffrey-Bailey, T. (2017). The urban heat island effect, its causes, and mitigation, with reference to the thermal properties of asphalt concrete. *Journal of Environmental Management*, *197*, 522–538. https://doi.org/10.1016/j.jenvman.2017.03.095

Muis, Sanne, Irazoqui Apecechea, Maialen, Dullaart, Job, Yan, Kun, de Lima Rego, Joao, Su, Jian, Madsen, Kristine S., & Verlaan, Martin. (2020). CoDEC Dataset - Data underlying the paper "A high-resolution global dataset of extreme sea levels, tides and storm surges including future projections " [Data set]. In *Frontiers of Marine Sciences*. Zenodo. https://doi.org/10.5281/zenodo.3660927

Muthusamy, M., Casado, M. R., Salmoral, G., Irvine, T., & Leinster, P. (2019). A remote sensing based integrated approach to quantify the impact of fluvial and pluvial flooding in an urban catchment. *Remote Sensing*, *11*(5). https://doi.org/10.3390/rs11050577

OECD. (2022). *Resilient Cities*. https://www.oecd.org/cfe/regionaldevelopment/resilient-cities.htmhttps://www.oecd.org/cfe/regionaldevelopment/resilient-cities.htm

Resilient Cities Network. (2022). The world's leading urban resilience network. https://resilientcitiesnetwork.org/network/

Sharifi, A., Chiba, Y., Okamoto, K., Yokoyama, S., & Murayama, A. (2014). Can master planning control and regulate urban growth in Vientiane, Laos? *Landscape and Urban Planning*, 131, 1–13. https://doi.org/10.1016/j.landurbplan.2014.07.014

Slager, K., A. Burzel, E.Bos, K. de Bruijn, D. Wagenaar, H. Winsemius, L. Bouwer, M. van der Doef (2016), User Manual Delft-FIAT version 1, website: www.publicwiki.deltares.nl/display/DFIAT/Delft-FIAT+Home

Sonnasinh, V. (2008). Lao PDR country flood report for 2008. *Integrated flood risk management in the Mekong River Basin*, 68-78.

Try, S., Sayama, T., Oeurng, C. *et al.* (2022). Identification of the spatio-temporal and fluvial-pluvial sources of flood inundation in the Lower Mekong Basin. *Geosci. Lett.* **9,** 5. https://doi.org/10.1186/s40562-022-00215-0

UN. (2022). 11 Make cities and human settlements inclusive, safe, resilient and sustainable. https://sdgs.un.org/goals/goal11

UN. (2022). 13 Take urgent action to combat climate change and its impacts. https://sdgs.un.org/goals/goal13

UNISDR. (n.d.). *Sendai Framework for Disaster Risk Reduction 2015-2030.*

Walsh, B., & Hallegatte, S. (2020). Measuring Natural Risks in the Philippines: Socioeconomic Resilience and Wellbeing Losses. *Economics of Disasters and Climate Change*, *4*(2), 249–293. https://doi.org/10.1007/s41885-019-00047-x

Ward, P. J., Winsemius, H. C., Kuzma, S., Bierkens, M. F. P., Bouwman, A., Moel, H. DE, … Luo, T. (2020). Aqueduct Floods Methodology. Technical Note. World Resources Institute.

Weilnhammer, V., Schmid, J., Mittermeier, I., Schreiber, F., Jiang, L., Pastuhovic, V., … Heinze, S. (2021). Extreme weather events in europe and their health consequences – A systematic review. *International Journal of Hygiene and Environmental Health*, *233*(August 2020). https://doi.org/10.1016/j.ijheh.2021.113688

Williams, T. G., Guikema, S. D., Brown, D. G., & Agrawal, A. (2020). Resilience and equity: Quantifying the distributional effects of resilience-enhancing strategies in a smallholder agricultural system. *Agricultural Systems*, *182*. https://doi.org/10.1016/j.agsy.2020.102832

WorldPop. (2022). Population counts. https://www.worldpop.org/project/categories?id=3

Acknowledgment

I would firstly like to thank Hans Gehrels for the opportunity given to explore this topic through the internship at Deltares, for its feedback and his enthusiasm throughout the whole experience. Following, I would like to thank Dr. Jaivime Evaristo for the academic and moral support provided during the more complicated steps of the research. A special thanks goes also to my colleagues from Deltares Bramka Jafino, Dirk Eilander, and Anaïs Couasnon for their help and patience concerning the technical aspects of the research and their useful feedback. Lastly, I am grateful for all the brainstorming, feedback and incredible support received by my peers Daniel and Jasper, and all the others who read this thesis.

Appendices

A GitHub folder (https://github.com/AliceAmpolini/Resilience-Quantification---Msc-Thesis.git) was created for 2 reasons. Firstly, it allows a better management of the input files as well as the software used during the research, and lastly, it provides an open solution to share the results and the research itself with academics.

Appendix A – QGIS Applications

All the shapefiles, vector and raster layers created in this research are available on the GitHub folder.

Getting the metropolitan subdistrict areas from a shapefile in QGIS

Once the shapefile is downloaded it can be opened on QGIS. Many layers open, however, only the once having the subdistricts are being saved. To isolate each subdistrict the 'select area by features' tool is used. Once the subdistricts are selected within the metropolitan borders they can be copied and pasted on a new layer.

Distributional Impacts and Beyond Design Event

Drag the resulting raster layer from Delft-FIAT on QGIS on the shapefile at the subdistricts level of the case study. Then, run zonal statistics between the merged shapefile and the damages, selecting the sum of damages. Give to the new vector layer colors on the shade of reds (classification). The resulting sum of damages per districts are then copy and pasted on Excel for further analysis.

To find the Distributional Impacts per capita the population raster is downloaded from WorldPop (data from 2020). The data (raster layer) is opened on QGIS to be submitted to zonal statistics with the merged subdistricts to find the sum of population that is further used in the analysis on Excel to find the sum of damages per subdistrict per capita.

Welfare loss

The dataset from Drayad (Kummu et al., 2020) called GDP_PPP_30arcsec_v3_nc was downloaded and opened on QGIS. Zonal statistics between the raster layer (band 3 representing the year 2015 was selected) and the merged subdistricts layer was ran to find the sum of the GDP PPP in the metropolitan area.

Appendix B – SFINCS Applications

The initial step are shown in the Appendix 1 and consisted in opening a command prompt (Miniconda3 was used for this research) and navigating to the folder in which the files of interest were kept and activating the model HydroMT SFINCS while launching the Jupyter notebook.

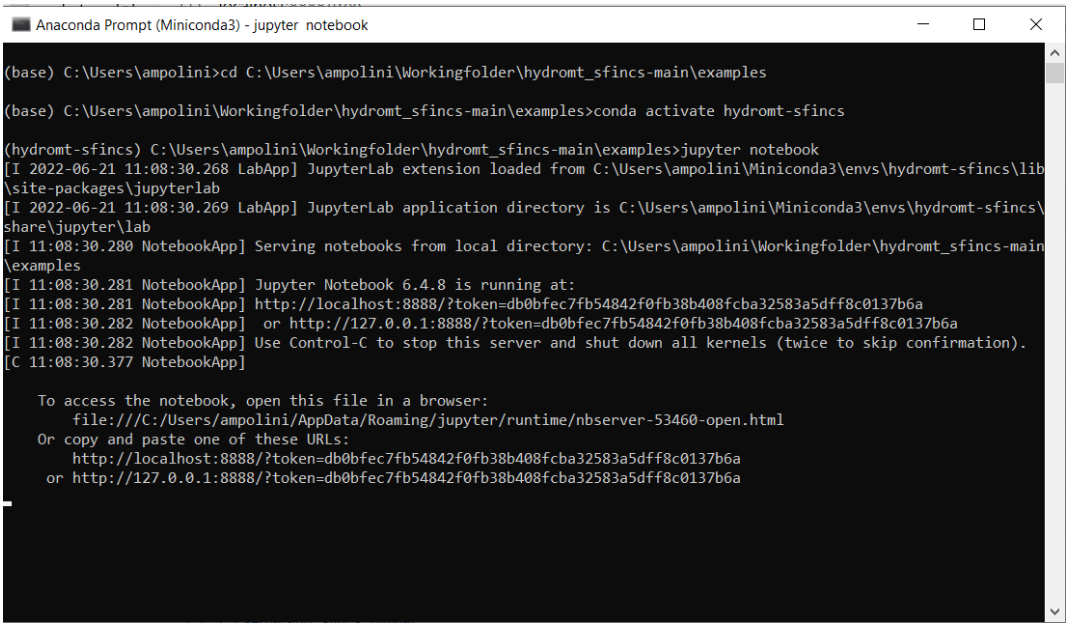

APPENDIX 1: THE FIGURE SHOWS THE STARTING COMMANDS RAN ON MINICONDA3 TO ACTIVATE THE MODEL AND OPEN THE JUPYTER NOTEBOOK

Then, a configuration file .ini was created for building or updating the models. These were .txt files saved into the main folder called in the Miniconda3 prompt.

All the input files (excel files and configuration files) and the notebooks can be found on the GitHub folder for the Recovery Time indicator and the modelled pluvial event of Semarang 50-years return period.

Appendix C – Delft-FIAT Applications

Delft-FIAT was ran directly on Miniconda3 by firstly activating HydroMT-FIAT (as previously shown in Appendix 1), then running the following lines to set up the model and generating raster layers that were analyzed on QGIS. The complete folder containing input and output files can be found on the GitHub folder.

for setting up FIAT
hydromt build fiat \path to the folder in which the model is built "{'grid': /path to the flooding extent from SFINCS file" -i \path to the configuration.ini file –dd (to access the Deltares archive)

for running FIAT (run inside the FIAT-model folder)
python \path to the fiat executable fiat.py -i \path to the second configuration .ini file generated while setting up the model

#Config. Vientiane pluvial rp 50
hydromt build fiat C:\Users\ampolini\Workingfolder\Alice-FIAT\Vientiane_pluvial_50 "{'grid': 'C:/Users/ampolini/Workingfolder/Alice-FIAT/Hazard/hmax_RP_50_vientiane_pluvial.tif'}" -i C:\Users\ampolini\Workingfolder\Alice-FIAT\configuration_vientiane_pluvial.ini --dd
python C:\Users\ampolini\Workingfolder\Alice-FIAT\fiat.py -i C:\Users\ampolini\Workingfolder\Alice-FIAT\Vientiane_pluvial_50\fiat_configuration.ini

#Config. Vientiane fluvial rp 100
hydromt build fiat C:\Users\ampolini\Workingfolder\Alice-FIAT\Vientiane_fluvial_100 "{'grid': 'C:/Users/ampolini/Workingfolder/Alice-FIAT/Hazard/hmax_RP_100_vientiane_fluvial.tif'}" -i C:\Users\ampolini\Workingfolder\Alice-FIAT\configuration_vientiane_fluvial.ini --dd
python C:\Users\ampolini\Workingfolder\Alice-FIAT\fiat.py -i C:\Users\ampolini\Workingfolder\Alice-FIAT\Vientiane_fluvial_100\fiat_configuration.ini

#Config. Semarang coastal rp 100

```
hydromt build fiat C:\Users\ampolini\Workingfolder\Alice-FIAT\Semarang_coastal_100 "{'grid':
'C:/Users/ampolini/Workingfolder/Alice-FIAT/Hazard/hmax_RP_100_semarang_coastal.tif'}" -i
C:\Users\ampolini\Workingfolder\Alice-FIAT\configuration_semarang_coastal.ini --dd
python C:\Users\ampolini\Workingfolder\Alice-FIAT\fiat.py -i C:\Users\ampolini\Workingfolder\Alice-
FIAT\Semarang_coastal_100\fiat_configuration.ini

#Config. Semarang coastal rp 1000
hydromt build fiat C:\Users\ampolini\Workingfolder\Alice-FIAT\Semarang_coastal_1000 "{'grid':
'C:/Users/ampolini/Workingfolder/Alice-FIAT/Hazard/hmax_RP_1000_semarang_coastal.tif'}" -i
C:\Users\ampolini\Workingfolder\Alice-FIAT\configuration_semarang_coastal_1000.ini --dd
python C:\Users\ampolini\Workingfolder\Alice-FIAT\fiat.py -i C:\Users\ampolini\Workingfolder\Alice-
FIAT\Semarang_coastal_1000\fiat_configuration.ini

#Config. Semarang pluvial rp 50
hydromt build fiat C:\Users\ampolini\Workingfolder\Alice-FIAT\Semarang_pluvial_50 "{'grid':
'C:/Users/ampolini/Workingfolder/Alice-FIAT/Hazard/hmax_RP_50_semarang_pluvial.tif'}" -i
C:\Users\ampolini\Workingfolder\Alice-FIAT\configuration_semarang_pluvial.ini --dd
python C:\Users\ampolini\Workingfolder\Alice-FIAT\fiat.py -i C:\Users\ampolini\Workingfolder\Alice-
FIAT\Semarang_pluvial_50\fiat_configuration.ini
```

Appendix D – Excel Applications

The Excel applications to the research can be found on the GitHub folder. It contains a document with the dashboard with the indicators for the two case studies and the sensitivity analysis.

Appendix E – Rstudio Applications

The following coding lines were ran to create the descriptive statistics of the research. The file can be found on the GitHub folder too.

```
#create a histogram and a boxplot for pluvial flooding in Semarang
v <- (as.numeric(Di_pluv_sem[,]))
hist(v, main = "", xlab = "", breaks = 7)
par = (new=T)
boxplot(v,horizontal=TRUE,outline=FALSE, ylim=c(0,0.2))
abline(v = median(v),                  # Add line for median
       col = "red",                                                    #Red and with width=5
       lwd = 5)
text(x = 0.09,               # Add text for median
     y = 5.5,
     paste("Median =", round(median(v), digits = 2)),
     col = "red",
     cex = 2)
#create a histogram and a boxplot with boxplot for coastal flooding in Semarang
v1 <- (as.numeric(unlist(DI_coastal[,])))
hist(v1, main = "", xlab = "", breaks = 7)
boxplot(v1,horizontal=TRUE,outline=FALSE, ylim=c(0,0.8))
abline(v = median(v1),                  # Add line for median
       col = "red",                                                    #Red and with width=5
       lwd = 5)
text(x = 0.2,               # Add text for median
     y = 3.5,
     paste("Median =", round(median(v1), digits = 2)),
     col = "red",
     cex = 2)
#create a histogram and a boxplot for pluvial flooding in Vientiane
vp <- (as.numeric(unlist(Vientiane_pluvial_di)))
hist(vp, main = "", xlab = "", xlim = c(0.05,0.3), breaks = 7)
boxplot(vp, horizontal = TRUE, outline = FALSE, ylim = c(0.05,0.3))
abline(v = median(vp),                  # Add line for median
       col = "red",                                                    #Red and with width=5
       lwd = 5)
text(x = 0.21,               # Add text for median
     y = 1.5,
     paste("Median =", round(median(vp), digits = 2)),
     col = "red",
     cex = 2)
#create a histogram and a boxplot for fluvial flooding in Vientiane
vf <- (as.numeric(unlist(vientiane_di_fluv[,])))
hist(vf, main = "", xlab = "", breaks = 7, xlim = c(0,0.5))
boxplot(vf, horizontal = TRUE, outline = FALSE, ylim = c(0,0.5))
abline(v = median(vf),                  # Add line for median
       col = "red",                                                    #Red and with width=5
       lwd = 5)
text(x = 0.21,               # Add text for median
     y = 1.5,
     paste("Median =", round(median(vf), digits = 2)),
     col = "red",
```

```
    cex = 2)
#create histogram and boxplot for semarang pluvial resilience
rsp <- (as.numeric(unlist(res_sem_pluv[,])))
par(mfrow=c(1,1))
hist(rsp, main ="Semarang Pluvial Flooding", xlab = "", breaks = 10, xlim = c(0,1))
                        # Draw histogram
abline(v = mean(rsp),                   # Add line for mean
       col = "red",
       lwd = 3)
text(x = 0.85,                  # Add text for mean
     y = 15,
     paste("Mean =", round(mean(rsp), digits = 2)),
     col = "red",
     cex = 2)
t.test(rsp)
#create histogram and boxplot for semarang coastal resilience
rsc <- (as.numeric(unlist(res_sem_coast[,])))
hist(rsc, main = "Semarang Coastal Flooding", xlab = "", breaks = 10, xlim = c(0,1))
abline(v = mean(rsc),                   # Add line for mean
       col = "red",
       lwd = 3)
text(x = 0.88,                  # Add text for mean
     y = 15,
     paste("Mean =", round(mean(rsc), digits = 2)),
     col = "red",
     cex = 2)
t.test(rsc)
#create histogram and boxplot for vientiane pluvial resilience
rvp <- (as.numeric(unlist(res_vient_pluv_vero[,])))
hist(rvp, main = "Vientiane Pluvial Flooding ", xlab = "", breaks = 10, xlim = c(0,1))
abline(v = mean(rvp),                   # Add line for mean
       col = "red",
       lwd = 3)
text(x = 0.85,                  # Add text for mean
     y = 15,
     paste("Mean =", round(mean(rvp), digits = 2)),
     col = "red",
     cex = 2)
t.test(rvp)
#create histogram and boxplot for vientiane fluvial resilience
rvf <- (as.numeric(unlist(res_vient_pluv[,])))
hist(rvf, main = "Vientiane Fluvial Flooding ", xlab = "", breaks = 10, xlim = c(0,1))
abline(v = mean(rvf),                   # Add line for mean
       col = "red",
       lwd = 3)
text(x = 0.55,                  # Add text for mean
     y = 15,
     paste("Mean =", round(mean(rvf), digits = 2)),
     col = "red",
     cex = 2)
t.test(rvf)
#create superimposed normalized curves of histograms
rvf2 <- seq(min(rvf), max(rvf), length = 101)
fun <- dnorm(rvf2, mean = mean (rvf), sd = sd(rvf))
plot(rvf2,fun, type = "l", col = "darkred", lwd = 3, xlim = c(0,1), ylim = c(0,4.2))
text(x = 0.39,
     y = 3,
     paste("(d)"),
     col = "darkred",
     cex = 2)

rvp2 <- seq(min(rvp), max(rvp), length = 101)
fun <- dnorm(rvp2, mean = mean (rvp), sd = sd(rvp))
lines(rvp2,fun, type = "l", col = "red", lwd = 3, xlab = "", ylab = "")
text(x = 0.55,
     y = 4,
     paste("(c)"),
     col = "red",
     cex = 2)

rsp2 <- seq(min(rsp), max(rsp), length = 101)
fun <- dnorm(rsp2, mean = mean (rsp), sd = sd(rsp))
lines(rsp2,fun, type = "l", col ="gold", lwd = 3, xlab = "", ylab = "")
text(x = 0.65,
     y = 3.2,
     paste("(a)"),
     col = "gold",
     cex = 2)

rsc2 <- seq(min(rsc), max(rsc), length = 101)
fun <- dnorm(rsc2, mean = mean (rsc), sd = sd(rsc))
lines(rsc2,fun, type = "l", col = "green", lwd = 3, xlab = "", ylab = "")
text(x = 0.68,
     y = 2.5,
     paste("(b)"),
     col = "green",
```

cex = 2)